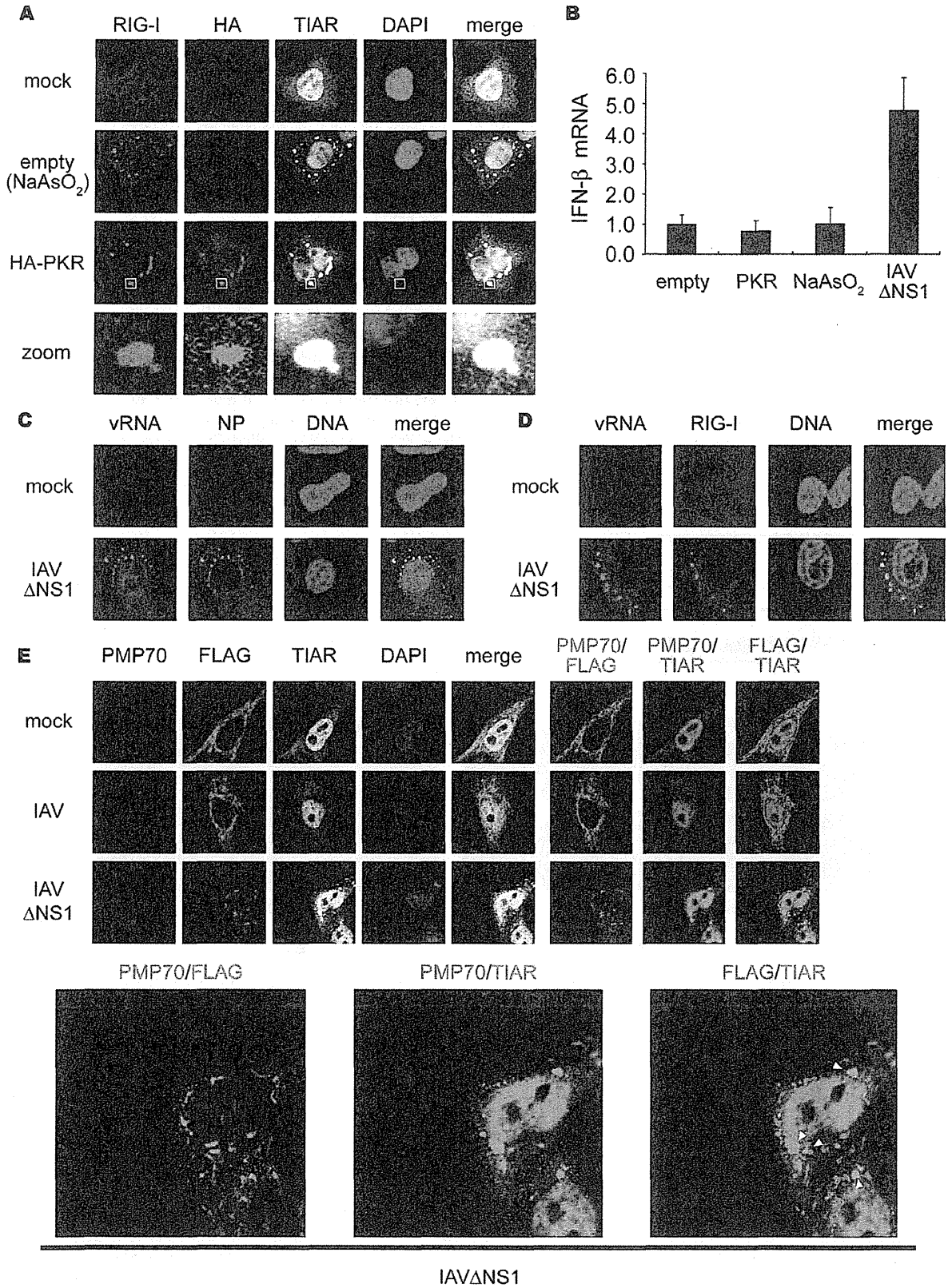
A
RIG-I
HA
TIAR
DAPI
merge
mock
empty (NaAsO2)
HA-PKR
zoom
B
IFN-β mRNA
6.0
5.0
4.0
3.0
2.0
1.0
0.0
empty
PKR
NaAsO2
IAV ΔNS1
C
vRNA
NP
DNA
merge
mock
IAV ΔNS1
D
vRNA
RIG-I
DNA
merge
mock
IAV ΔNS1
E
PMP70
FLAG
TIAR
DAPI
merge
PMP70/ FLAG
PMP70/ TIAR
FLAG/ TIAR
mock
IAV
IAV ΔNS1
PMP70/FLAG
PMP70/TIAR
FLAG/TIAR
IAVΔNS1

Figure 3. Viral RNA is required for formation of functional SG to activate RIG-I/IPS-1 signaling pathway. (**A**) 293T cells were transfected with empty vector (empty) or the HA-PKR expression vector (HA-PKR) for 24 h, or treated with $NaAsO_2$ for 1 h and stained with anti-RIG-I, anti-HA (PKR) and anti-TIAR antibodies and DAPI. The zoomed images correspond to the boxed regions. (**B**) 293T cells were transfected with empty vector (empty), or the HA-PKR expression vector for 48 h, or treated with $NaAsO_2$ for 1 h, or infected with IAVÄNS1 for 12 h. Relative mRNA levels of endogenous IFN-â gene were determined by quantitative PCR (qPCR). Data are represented as the mean standard ± error of the mean (SEM). (**C and D**) HeLa cells were mock-treated or infected with IAVÄNS1 for 12 h. Viral RNA (vRNA) was detected by the FISH method using an RNA probe complementary to the segment 1 of the IAV, and NP (**C**) and RIG-I (**D**) were detected using anti-NP and anti-RIG-I antibodies (97.1%, and 98.2% colocalization of vRNA with NP and RIG-I, respectively). TO-PRO-3 was used for staining of nuclear DNA (DNA). (**E**) HeLa cell lines stably expressing FLAG-tagged IPS-1 were mock-treated or infected with IAV or IAVÄNS1 for 10 h. The cells were stained with anti-PMP70, anti-FLAG, and anti-TIAR antibodies. The white arrowheads indicated the contacts between FLAG-IPS-1 and TIAR. 67.8% of IAVÄNS1 infected cells exhibited contacts, whereas IAV infected cells hardly exhibited the contact (2.7%). The zoomed images of PMP70 (Green) and FLAG (Red), PMP70 (Green) and TIAR (Red), and FLAG (Green) and TIAR (Red) in IAVÄNS1-infected cells were shown in the bottom panel.
doi:10.1371/journal.pone.0043031.g003

Critical Role of PKR in avSG Formation and IFN Production in IAV-infected Cells

The results described above indicate the formation of viral RNA-containing avSGs to be essential to RLR-mediated antiviral signaling. To evaluate the requirement of PKR during IAVÄNS1 infection, we analyzed the formation of avSGs in mouse embryonic fibroblasts (MEFs) derived from WT and PKR knock-out (KO) mice (Figure 6). PKR WT and KO MEFs were infected with either IAV or IAVÄNS1, and stained with the anti-RIG-I, anti-NP, and anti-TIAR antibodies and calculated the frequency of avSGs. In the case of WT IAV, avSGs did not form in WT and KO MEFs as determined in Figure 1. IAVÄNS1 produced avSGs in WT but not in PKR KO MEFs (Figure 6A, 6B, 6C). Moreover, deletion of PKR resulted in a blockade of IFN-â gene expression (Figure 6D), production of IFN-â protein (Figure 6E), and IRF-3 dimerization (Figure 6F). Furthermore, we confirmed these results using siRNA targeting PKR expression in HeLa cells. The siRNA efficiently knocked down endogenous

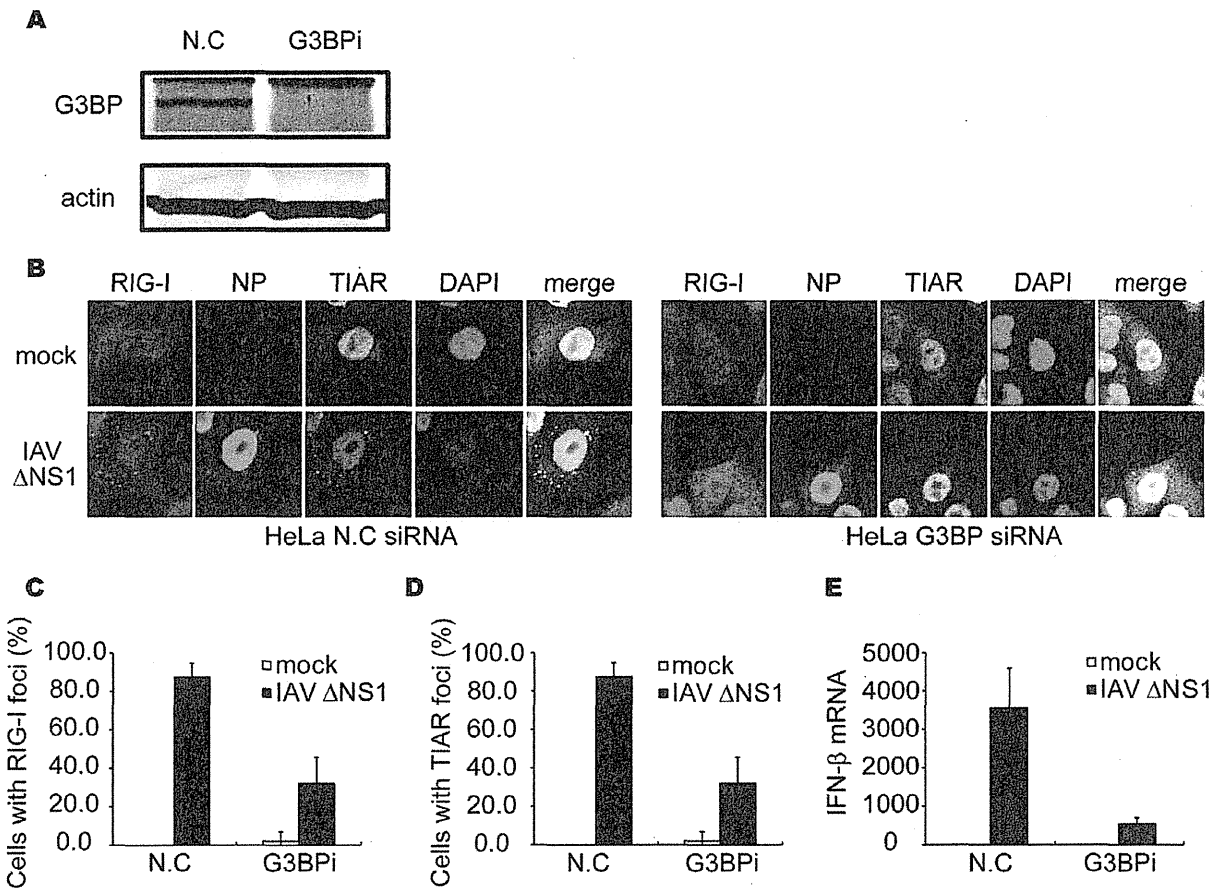

Figure 4. Knockdown of G3BP impairs formation of avSG and IFN-â gene activation. (**A–E**) HeLa cells were transfected with control siRNA (N.C) or siRNA targeting human G3BP (G3BPi). At 48 h after transfection, cells were harvested and G3BP and actin were detected by immunoblotting (**A**). Cells were mock-treated (mock) or infected with IAVÄNS1 for 12 h and fixed and stained with anti-RIG-I, anti-NP and anti-TIAR antibodies and DAPI (**B**). The percentage of cells containing foci of RIG-I (**C**) or TIAR (**D**) was determined. Relative mRNA level of IFN-â was determined by qPCR (**E**). Data are represented as the mean standard ± error of the mean (SEM).
doi:10.1371/journal.pone.0043031.g004

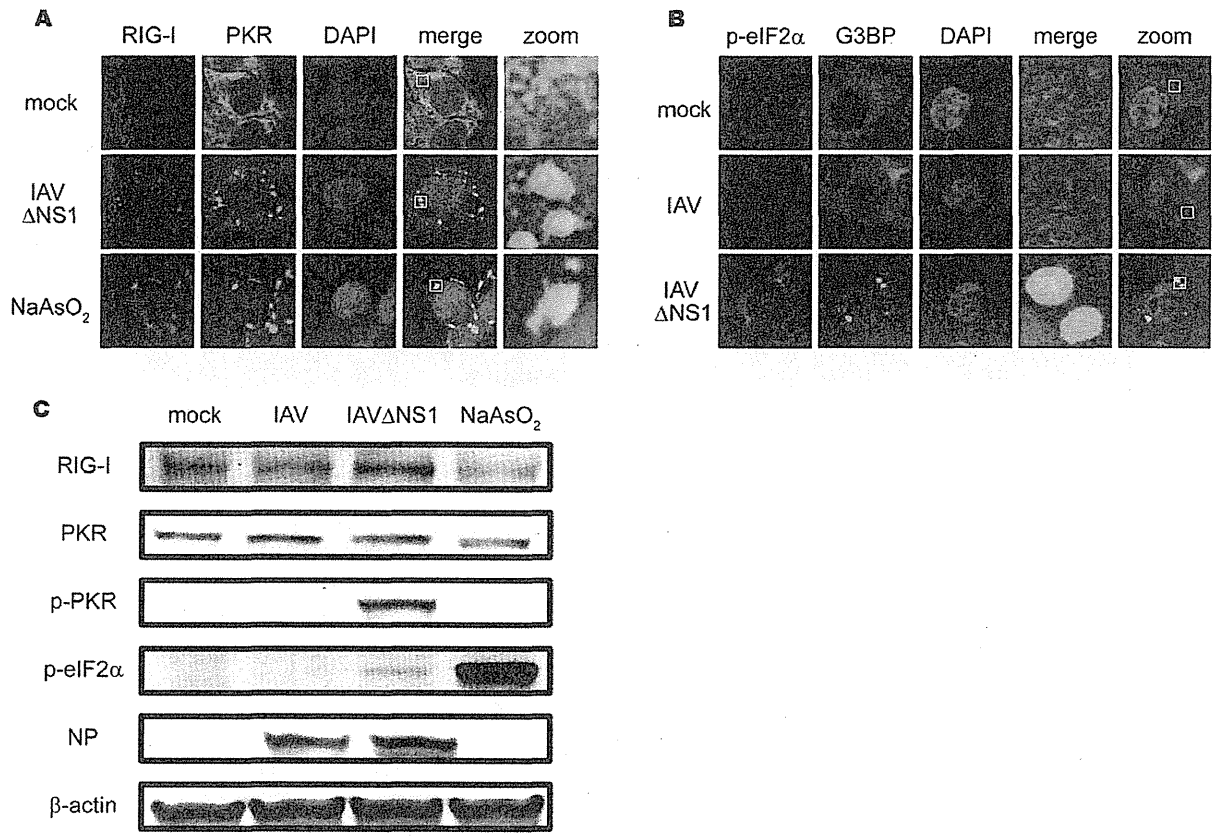

Figure 5. Localization and activation of PKR in IAVÄNS1-induced avSGs. (**A**) HeLa cells were mock-treated or infected with IAVÄNS1 for 9 h or treated with $NaAsO_2$ for 1 h. Cells were fixed and stained with anti-RIG-I and anti-PKR antibodies (% of colocalization: 95.1% and 97.0% in IAVÄNS1-infected and $NaAsO_2$-treated cells, respectively). The zoomed images correspond to the boxed regions. (**B**) HeLa cells were mock-treated or infected with IAV or IAVÄNS1 for 9 h and stained with anti-phospho-eIF2á (Ser 51) (p-eIF2á) and G3BP (% colocalization: 0.0% and 46.5% in IAV and IAVÄNS1-infected cells, respectively). The zoomed images correspond to the boxed regions. (**C**) HeLa cells were infected with IAV or IAVÄNS1 for 12 h or treated with $NaAsO_2$ for 1 h. Cell extracts were prepared and subjected to SDS-PAGE, and immunoblotted using antibodies against RIG-I, PKR, phosphorylated PKR (Thr 446) (p-PKR), phosphorylated eIF2á (Ser 51) (p-eIF2á), IAV NP, and â-actin.
doi:10.1371/journal.pone.0043031.g005

PKR expression, resulting in a strong inhibition of the IAVÄNS1-induced IFN-â gene expression, concomitant impairment of the number of avSG (Figure S6). Taken together, the results indicate that PKR is essential for avSGs and IFN gene activation in IAVÄNS1-infected cells. Importantly, blocking avSG formation by knockdown of PKR or G3BP enhanced the replication of IAVÄNS1 (Figure 7). These results strongly indicate a novel role for avSGs in the antiviral innate immune responses.

It is worth to note that in the absence of PKR, cytoplasmic transport of NP is accelerated (Figure 6A). This effect is also observed in HeLa cells in which PKR is knocked down (Figure S6C). Although the mechanism is unknown, these results suggest that PKR negatively regulate cytoplasmic transport of IAV nucleocapsid.

Viral RNA Generates avSGs in a PKR-dependent Manner

Previous reports showed that genomic RNA of IAV is responsible for triggering antiviral signaling via RIG-I [6,9,24,25]. Because the IAV genome is not infectious, we extracted it from the IAV-infected cells and transfected it into WT or PKR KO MEFs, and investigated whether the IAV genomic RNA solely induces the formation of avSGs and subsequent activation of the IFN gene. As shown in Figure 8A, the IAV genomic RNA is sufficient to produce avSGs, indicating that neither viral protein nor viral RNA replication is required. Furthermore, PKR is required for the formation of viral RNA-induced avSGs (Figure 8A and 8B). Because PKR is also required for poly I:C-induced IFN gene activation [26], we tested short and long poly I:C, which selectively activate RIG-I and MDA5, respectively [27]. Short and long poly I:C induced the formation of avSGs in a PKR-dependent manner (Figure 8A and 8B). We confirmed that IFN-â production by these RNA is PKR-dependent (Figure 8C). Viral but not host RNA is capable of triggering the response, as demonstrated by the finding that total RNA extracted from infected cells but not uninfected cells induced the formation of avSGs and activation of the IFN-â gene (Figure S7A and S7B). These findings demonstrate that PKR is necessary for formation of avSGs which recruits viral RNA and RLRs to trigger IFN gene activation during the IAV-infection. Of note, as shown in Figure 3B, overexpression of PKR can activate SG formation but not IFN expression in the absence of viral RNA, suggesting that function of PKR is prerequisite but insufficient for efficient induction of RLR-mediated antiviral signaling.

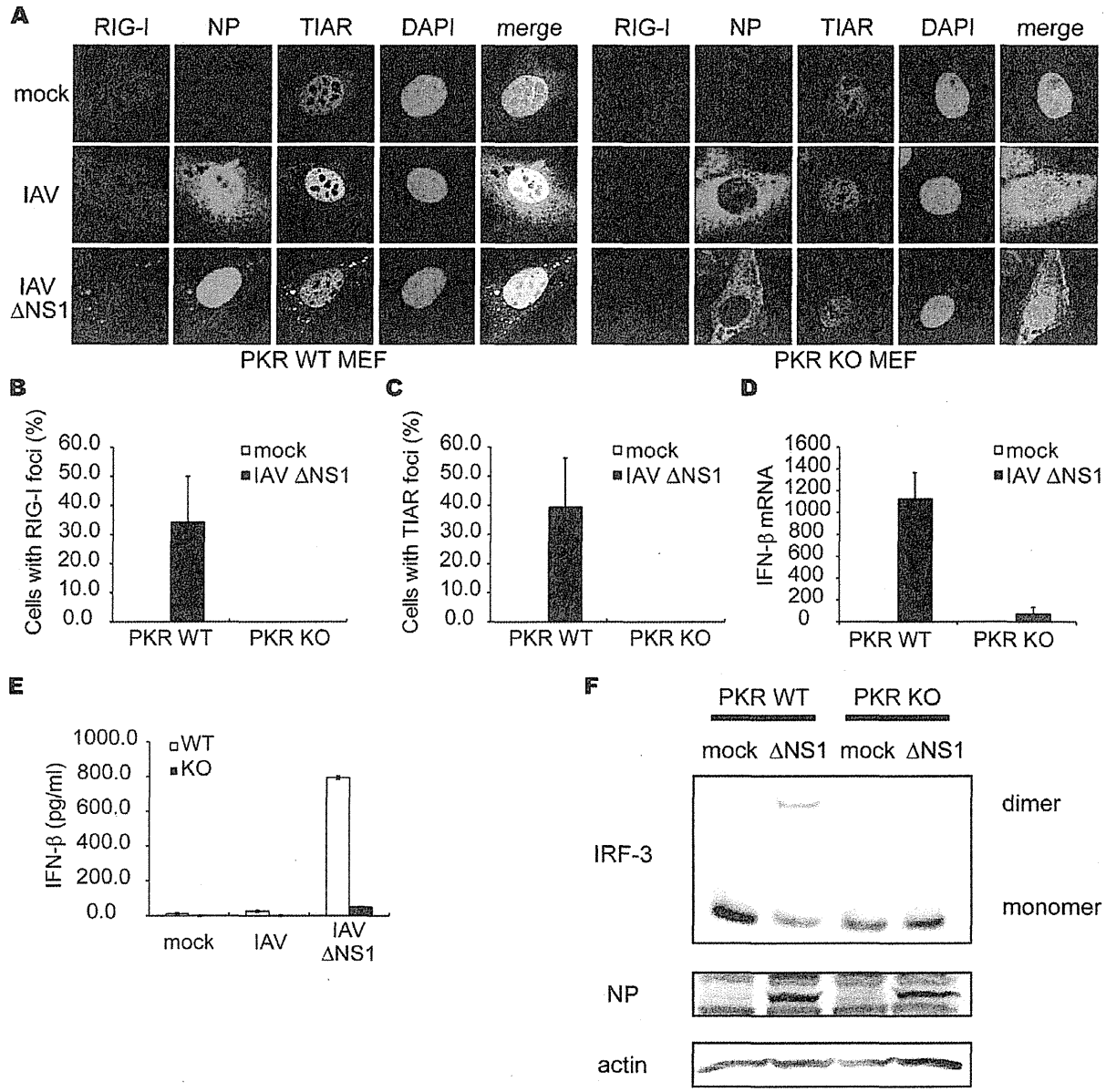

Figure 6. Critical role of PKR in formation of avSG and IFN-â gene activation. (**A–C**) MEFs derived from WT and PKR KO mice were mock-treated or infected with IAVÄNS1 for 12 h. The cells were stained with anti-RIG-I, anti-IAV NP and anti-TIAR antibodies and DAPI (**A**). The percentage of cells containing foci of RIG-I (**B**) or TIAR (**C**) was determined. (**D–F**) PKR WT and PKR KO MEFs were mock-treated or infected with IAVÄNS1. The IFN-â mRNA level at 9 h post-infection was determined by qPCR (**D**). The IFN-â protein levels in culture medium at 15 h post-infection were quantified by ELISA (**E**). Cell extracts were subjected to Native-PAGE and IRF-3 dimer was detected by immunoblotting using anti-IRF-3 antibody. IAV NP and actin were detected by SDS-PAGE followed by blotting using anti-NP and anti-actin antibodies (**F**). Data shown in B-E are represented as the mean standard ± error of the mean (SEM).
doi:10.1371/journal.pone.0043031.g006

Discussion

Recent studies have identified the domain structure of RLRs and the various adaptor proteins regulating RLR-mediated antiviral signaling cascades [28], but how RLRs encounter viral RNA in infected cells remain unclear. In this study, we found that all RLRs are recruited into cytoplasmic granules, termed avSGs, upon viral infections. avSGs contain many SG markers, G3BP, TIAR, and eIF3, but unlike canonical SGs, also contained viral RNA and viral NP. We demonstrated that avSGs are critical to virus-induced IFN gene activation. Since RLRs must efficiently find their ligands to act as vital sensors for viral RNA, avSGs may facilitate a proper encounter between viral RNA and RLRs. In addition, OAS and RNase L are recruited to avSGs, supporting the model that RNase L amplifies IFN-inducing signaling by unearthing cryptic ligands for RIG-I and MDA5 [29]. Further-

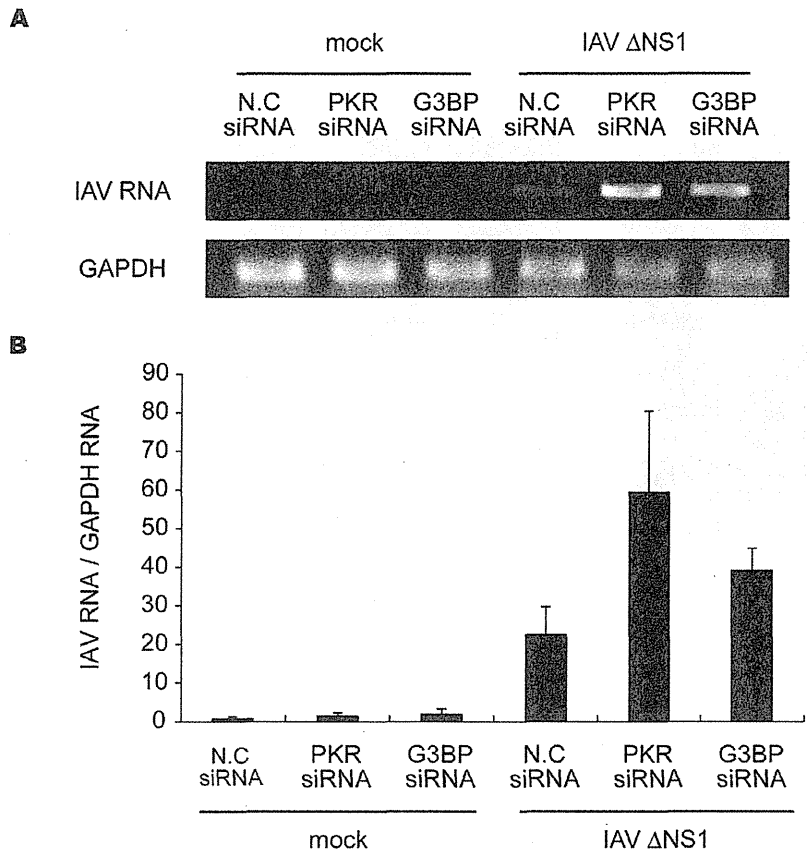

Figure 7. Inhibition of avSG formation enhanced IAV viral replication. HeLa cells were transfected with control siRNA (N.C) or siRNA targeting human PKR mRNA or G3BP. At 48 h after transfection, cells were mock-treated or infected with IAVÄNS1 for 24 h. The expression levels of IAV RNA segment 3 and GAPDH mRNA were determined by RT-PCR (**top**). The IAV RNA expression patterns were quantified with LAS-1000 UV mini (Fujifilm, Japan) and normalized with GAPDH (**bottom**). Data are represented as the mean standard ± error of the mean (SEM).
doi:10.1371/journal.pone.0043031.g007

more, the specific recruitment of antiviral proteins in avSGs suggests a critical role in the blocking of viral replication without an effect on host normal translation. We also observed that other viruses including SINV, EMCV Adenovirus, Hepatitis C virus and Newcastle disease virus induced avSG (Figure S5C and data not shown), suggesting that avSGs may function as a general platform for detection of many viruses to initiate antiviral signaling. Because PKR alone cannot trigger IFN gene activation (Figure 3B), PKR contributes at upstream of IAV-induced RIG-I activation. It was reported that SINV activates GCN2 to phosphorylate eIF2á [30], suggesting that the several viruses may activate different eIF2á kinases to form avSG.

Our model for the function of avSGs is summarized in Figure 9. We do not strictly rule out a possibility that PKR may directly phosphorylate target molecules to participate IFN gene activation, however because activation of PKR alone is not sufficient to trigger IFN production, this effect may be incremental.

Recognition of viral RNA by RIG-I and MDA5 induces ATP-dependent conformational change of the molecules and allows them to interact with mitochondrial IPS-1 via CARD-CARD interaction. Several reports indicated that activated RIG-I forms dimer or oligomer, which is required for efficient signal activation [31,32]. Furthermore, it was demonstrated that IPS-1 is redistributed on mitochondria in response to viral infection and IPS-1 forms prion-like aggregates [12,16]. These observations suggest a possibility that local enrichment of both RLRs and IPS-1 is required for signaling. Although our attempt to detect biochemical interaction between RLR-containing avSG and IPS-1 aggregates *in vitro* has been unsuccessful so far because of insoluble property of them, our immunohistochemical analysis strongly indicates that IPS-1-enriched mitochondria are physically attached with avSG in response to IAVÄNS1 infection (Figure 3E and S4), suggesting critical role of avSG as a platform for RLR-IPS-1 interaction.

The phosphorylation of eIF2á at Ser51 is known to trigger the formation of canonical SGs, however the precise mechanism by which the phosphorylated eIF2á recruits other SG components is not well understood because of difficulty of biochemical analysis [33]. We demonstrated that PKR was activated, recruited to avSGs, and essential for avSGs to form after IAVÄNS1 infection. Viral RNA is primarily responsible for triggering the PKR activation because transfection of IAV genomic RNA or poly I:C induced avSG formation and IFN gene activation in a PKR-dependent manner. Consistent with our data, some studies revealed that PKR deficiency impair production of IFN in response to polyI:C and viral infections [34–38]. Schulz et al. reported that PKR is not required for production of IFN-á/â proteins in response to IAV in bone marrow-derived dendritic cells (BM-DCs) [39]. This is apparently inconsistent with our data

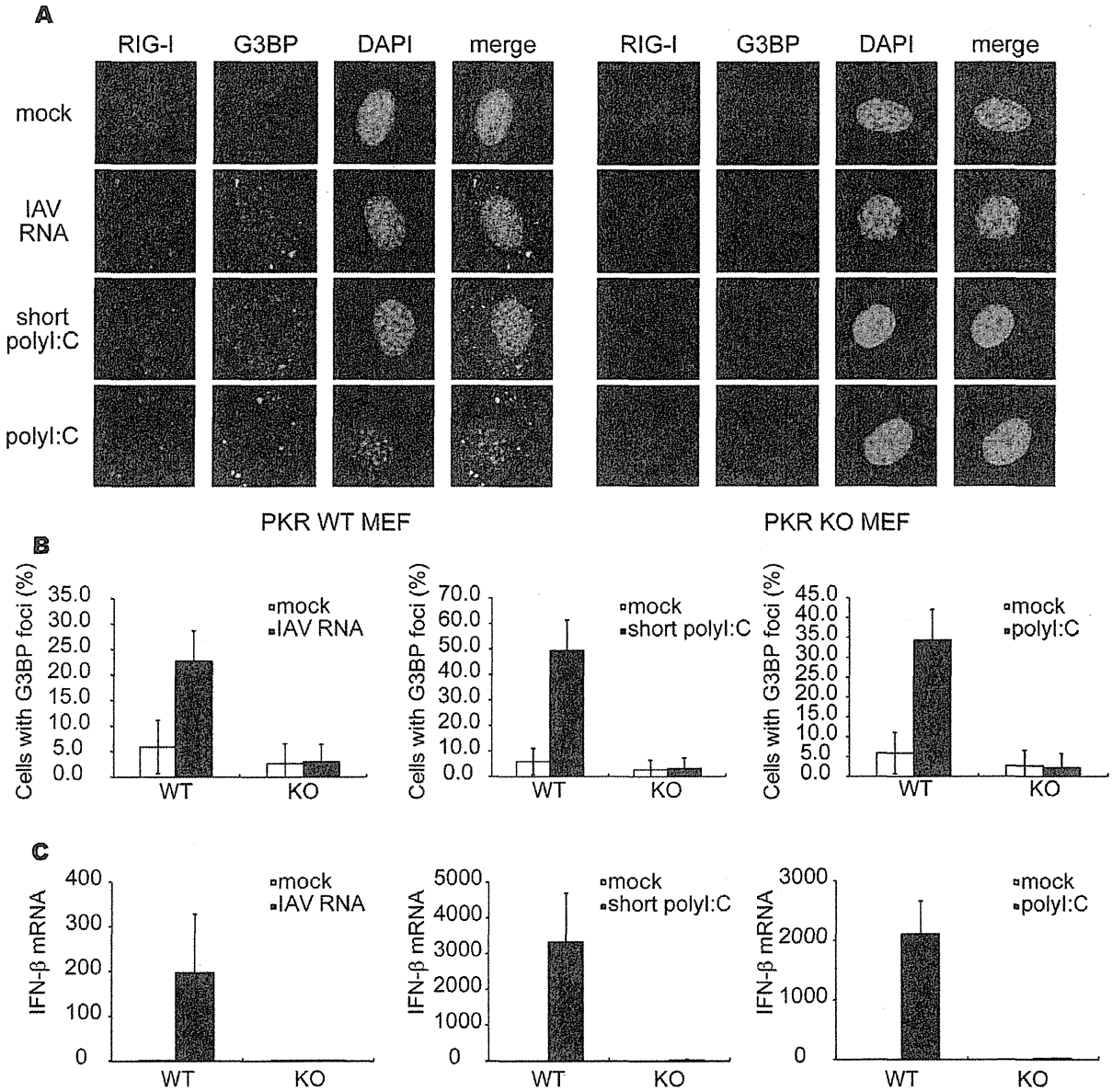

Figure 8. Viral RNA and polyI:C induce formation of avSGs and IFN-â gene expression in a PKR-dependent manner. (**A–C**) MEFs derived from WT and PKR KO mice were mock-treated or transfected with IAV genomic RNA, short poly I:C or long poly I:C for 9 h and stained with anti-RIG-I, anti-G3BP antibodies and DAPI (**A**). The percentage of cells containing foci of G3BP was shown in (**B**). Relative IFN-â mRNA levels were determined by qPCR (**C**). Data shown in B and C are represented as the mean standard ± error of the mean (SEM).
doi:10.1371/journal.pone.0043031.g008

obtained with MEFs. Although we were unable to directly compare between MEF and BM-DC, our explanation for this discrepancy is cell type difference, because IFN protein expression as determined by ELISA (Figure 6E) is consistent with mRNA level (Figure 6D) and PKR knockdown with HeLa cells dramatically diminished IFN production (Figure S6B). BM-DC may utilize eIF2á kinase other than PKR to form avSG.

The NS1 of IAV is a multifunctional protein that inhibits various host factors, including PKR [40,41], RIG-I [42,43], and tripartite motif-containing protein 25 (TRIM25), known to regulate RIG-I activation [44], and potentially sequesters viral dsRNA through its dsRNA-binding domain. Here, we demonstrated that NS1 of IAV markedly inhibited avSGs and the IFN gene's activation. Consistently, a recent report demonstrated that formation of IAV-induced SG was inhibited by wild type NS1, but not by mutant NS1, in which Arg38 and Arg41 are substituted to Ala [41]. Several classes of viruses are known to inhibit the formation of SGs during infection. The West Nile and Sendai viruses encode RNA that interacts with TIAR and inhibits SG assembly [45,46]. The poliovirus 3C protease cleaves G3BP at Gln 326 during the infection process [22]. Moreover, Simpon-Holley et al. recently demonstrated that the E3L protein of Vaccinia virus

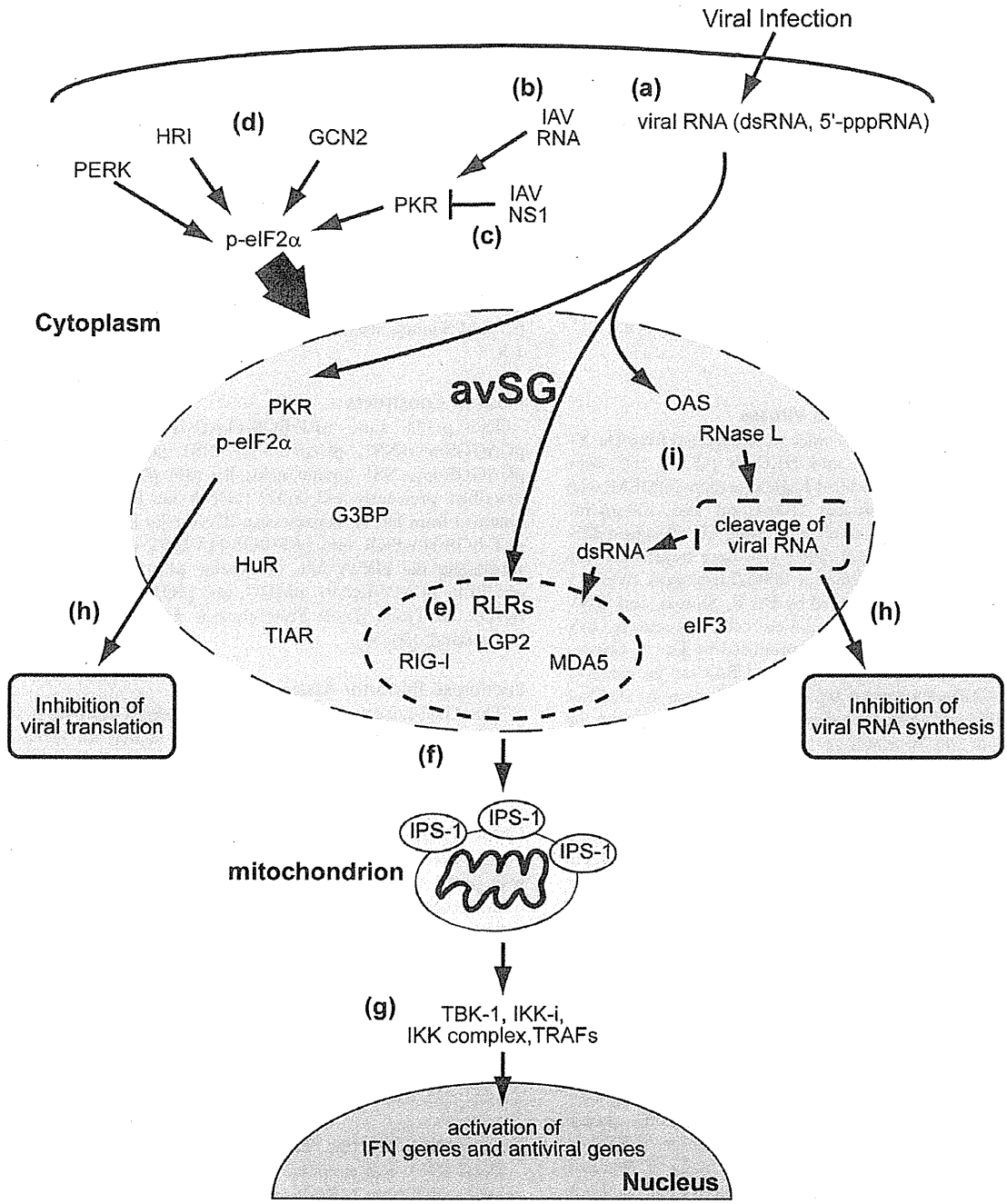

Figure 9. avSGs and innate antiviral responses. Viral infections generate RNA with non-self-signatures such as a 5′-tri-phosphate or double-stranded structure (**a**). In the case of IAVΔNS1, PKR is critical for the formation of avSGs (**b**). Wild-type IAV inhibits formation of avSGs by the actions of the NS1 protein (**c**). Some other viruses may activate different eIF2á kinases, such as GCN2, PERK, and HRI, to produce functional avSGs (**d**). avSGs are composed of SG markers and other RNA-binding proteins including RLRs, antiviral proteins (PKR, OAS, and RNase L) and viral RNA. Within avSGs, viral RNA could be sensed by RLRs to trigger antiviral signaling (**e**). Activated RLRs recruit mitochondrial IPS-1 via CARD-CARD interactions (**f**). IPS-1 serves as another platform for TRAFs and protein kinases, TBK-1, IKKi and IKK complex, to activate target genes (**g**). The antiviral proteins are activated by viral RNA to block viral RNA synthesis and translation (**h**). Moreover, OAS-RNase L system may produce dsRNA to amplify the RLR signaling (**i**).
doi:10.1371/journal.pone.0043031.g009

preventing PKR activation and phosphorylation eIF2á and the Vaccinia virus ÄE3L, lacking E3L genes, generated a granular-like structure distinguished from a granule termed antiviral granule (AVG) [47]. They also reported that MEFs lacking the AVG component TIA-1 exhibited increased Vaccinia viral replication, suggesting that AVG is critical for antiviral host responses. These

results strongly suggest that viruses acquire means to inhibit the formation of avSGs and subsequent activation of the IFN gene.

The canonical SG has been proposed as a storage compartment for translation-stalled host mRNA in response to various stresses and possible partner with another RNP complex, processing body, which is responsible for mRNA degradation [33]. Therefore, SG has been considered as a compartment for dynamic translational regulation upon environmental stress. Our findings discover a new role for newly identified avSG as a platform for interaction between viral RNA and host antiviral molecules to trigger a cascade of events leading to eradication of the virus. Although the difference between SG and avSG is not fully understood at this point, future research will delineate mechanism of their assembly and biological functions in stresses and immune responses.

Materials and Methods

Cell Culture, Transfection, and Viruses

MEFs from *pkr* +/+ and −/− mice were obtained from Dr. Yi-Li Yang [26]. HeLa, 293T, and HEC-1B [48,49] cells were maintained in Dulbecco's modified Eagle's medium (DMEM) with FBS and penicillin-streptomycin (100 U/ml and 100 μg/ml, respectively). HeLa cell line stably expressing FLAG-tagged IPS-1 was described previously [12]. 293T cells were transfected with FuGENE6 (Roche) or Lipofectamine 2000 (Invitrogen). Adenovirus type 12 (Ad12) dl203, provided by Dr. K. Shiroki, and SINV were propagated in 293T cells and Vero cells, respectively. IAV (A/PR/8/34 and ÄNS1), originally produced by Dr. A. Garcia-Sastre (Mount Sinai School of Medicine, USA) and provided by Dr. S. Akira (Osaka University, Japan), were grown in the allantoic cavities of 9-day-old embryonated eggs. Cells were treated with the culture medium ('mock-treated') or infected with IAV, IAVÄNS1, SINV, EMCV, or Ad12 dl203 in serum-free and antibiotic-free medium. After adsorption for 1 h at 37°C, the medium was changed and infection was continued for various periods in the presence of serum-containing DMEM. IAV genomic RNA was extracted from partially purified virus stock by TRIzol (Invitrogen) and 1.0 μg of viral RNA was transfected with Lipofectamine RNAi MAX (Invitrogen) in a 35 mm dish. PolyI:C was purchased from Amersham. Short polyI:C was prepared as described previously [27].

Immunoblotting, Antibodies and Reagents

The preparation of cell extracts and immunoblotting have already been described previously [5,50]. The polyclonal antibody used to detect human IRF-3 in native PAGE and anti-human and anti-mouse IRF-3 polyclonal antibodies for immunostaining were described previously [50]. The monoclonal antibody against Influenza NP (mAb61A5), which was generated by Dr. Y. Kikuchi (Iwaki Meisei University, Japan), was provided by Dr. F. Momose (Kitasato University, Japan) [51]. The monoclonal antibody against human OAS (6-1) was provided by Dr. Y. Sokawa (Kyoto Institute of Technology, Japan). The anti-human RIG-I, anti-human MDA5, and anti-human LGP2 antibodies were originally generated by immunizing rabbits with a synthetic peptide corresponding to amino acids 793–807 of human RIG-I, 145–160 of human MDA5, and 535–553 of human LGP2, respectively. As shown in Figure S1, knockdown of endogenous RIG-I by shRNAs specifically inhibit granule-like accumulation of RIG-I in immunostaining (Figure S1A) and appearance of band corresponding endogenous RIG-I in western blotting (Figure S1B), indicating high specificity of the anti-RIG-I antibody. Furthermore, a similar staining pattern was obtained with a monoclonal antibody for human RIG-I produced by Perseus Proteomics Inc, Japan. Other antibodies were obtained from the following sources: anti-G3BP (611126) from Transduction Laboratories™, anti-IRF-3 (CBX00167) from COSMO BIO, anti-PKR (sc-6282), anti-RNase L (sc-22870), anti-G3BP (sc-70283), anti-eIF3 (sc-16377), anti-c-myc (sc-40) and anti-TIAR (sc-1749) from Santa Cruz Biotechnology, anti-FLAG (M2) from Sigma, anti-phospho-PKR (pT446) (1120-1) from Epitomics, anti-actin (MAB1501R) from CHEMICON International, anti-PMP70 (ab3421) from Abcam, anti-HA-Tag (6E2) and anti-phospho-eIF2á (Ser51) (119A11) from Cell Signaling, and anti-HuR (RN004P, RIP-Certified antibody) and anti-â-actin (PM053) from MBL. Alexa 488-, 594-, and 633-conjugated anti-mouse, anti-rabbit, or anti-goat IgG antibodies purchased from Invitrogen were used as secondary antibodies. 0.5 mM Sodium arsenite (Sigma) was added to the cell culture for 1 h.

Plasmid Constructs

The p-125 Luc, pEF-BOS-FLAG-IPS-1, pCAGGS-myc, pCAGGS-myc-NS1, pCAGGS-myc-NS1 (amino acids 1–80), pCAGGS-myc-NS1 (amino acids 81–230) plasmids have been described previously [42,48,52]. cDNA for human PKR was obtained from Dr. A. Hovanessian (University Paris, France) and pEF-BOS-HA-PKR and pEF-BOS-HA-IPS1 were obtained by subcloning the cDNA into the vector pEF-BOS, respectively. pSUPER, pCMVÄR8.91, pMDG, and pRDI292 were provided by Dr. D. Trono (Ecole Polytechnique Federale de Lausanne, Switzerland) [53–56].

Luciferase Reporter Assay

The Dual-Luciferase Reporter Assay System (Promega) was used according to the manufacturer's instructions for luciferase assays. As an internal control, the *Renilla* Luciferase construct pRL-TK (Promega) was used.

Immunofluorescence Microscopy

Cells were fixed with 4% paraformaldehyde (PFA) for 20 min at 4°C, permeabilized with 0.05% Triton X-100 in PBS for 5 min at room temperature (RT), blocked with 5 mg/ml BSA in PBST (0.04% Tween20 in PBS) for 30 min, and incubated with relevant primary antibodies diluted in blocking buffer overnight at 4°C. The cells were then incubated with secondary antibodies for 1 h at RT. Nuclei were stained with 4.6-dimaidino-2-phenylinodole (DAPI) and analyzed with a confocal laser microscope, LSM 510-V4.2 (Carl Zeiss) or TCS-SP (Leica). The percentages of avSG-containing cells were calculated in more than 5 randomly chosen fields for each slide.

Quantitative Reverse Transcription-PCR

Total RNA was prepared with TRIzol reagent (Invitrogen), treated with DNase I (Roche Applied Science), and amplified by reverse transcription-PCR with the ABI PRISM 7700 sequence detection system (Applied Biosystems). TaqMan reverse transcription reagents (Applied Biosystems) were used for cDNA synthesis. We used commercial TaqMan Universal PCR Master Mix and TaqMan primer-probe sets (Applied Biosystems) for human and mouse IFN-â. As an internal control for the comparative threshold cycle methods, a primer-probe set for eukaryotic 18 s rRNA (Applied Biosystems) was used. The results were normalized to the abundance of internal control. For the detection of IAV RNA and glyceraldehyde-3-phophate dehydrogenase (GAPDH), we used specific primer sets and amplified with Ex Taq HS (Takara). IAV RNA: 5¢- ATTTGCAACACTACAGGGGC-3¢ (forward) and

5¢-GACTGACGAAAGGAATCCCA-3¢ (reverse). GAPDH mRNA:

5¢- GAGTCAACGGATTTGGTCGT-3¢ (forward) and

5¢- TTGATTTTGGAGGGATCTCG-3¢ (reverse).

Co-immunoprecipitation

The RIG-I antibody was cross-linked to Dynabeads protein G (Invitrogen) according to the manufacturer's protocol. Cell lysate was incubated with the anti-RIG-I antibody -Dynabeads for 120 min at RT. RIG-I-immunoprecipitated complexes were eluted by boiling in loading buffer and then processed for Western blotting.

RNA Interference

A lentiviral shRNA expression system was used. RIG-I shRNA#1 and RIG-I shRNA#2 were originally constructed. Oligonucleotides with the following sense and antisense sequences were used for the construction of the small hairpin RNA (shRNA)-encoding lentiviral vector. RIG-I shRNA#1; 5¢-GATCCCC-GAGGTGCAGTATATTCAGGTT CAAGAGACCTGAATA-TACTGCACCTCTTTTTGGAAA-3¢ (sense) and 5¢-AGCTT T TCCAAAAAGAGGTGCAGTATATTCAGGTCTCTT-GAACCTGAATATACTG CACCTCGGG-3¢ (antisense). RIG-I shRNA#2; 5¢-GATCCCCGAATTTAAAACCA GAAT-TATCTTCAAGAGAGATAATTCTGGTTT-TAAATTCTTTTTGGAAA-3¢ (sense) and 5¢-AGCTTTTC-CAAAAAGAATTTAAAACCAGAATTATCTCTC TTGAA-GATAATTCTGGTTTTAAATTCGGG-3¢ (antisense). The oligonucleotides described above were annealed and subcloned into the Bgl II-Hind III site of pSUPER. To construct the pLV-shRNA against RIG-I, the BamHI-SalI fragments excised from pSUPER-RIG-I#1 and pSUPER-RIG-I#2 were subcloned into the BamHI-SalI site of pRDI292. The recombinant lentiviruses were generated by transfection of the empty lentiviral vector, or respective shRNA construct together with the packaging construct pCMVÄR8.91 and the envelop plasmid pMDG. At 48 h after, the culture supernatant was collected and the medium filtered with a 0.45-μm filter was transferred, to HeLa cells. After 72 h, the cells were selected with medium containing 2 μg/ml of Puromycin (Sigma). The siRNA negative control and siRNAs targeting PKR and G3BP were purchased from Invitrogen. Each siRNA was transfected with Lipofectamine RNAi MAX (Invitrogen) according to the manufacturer's instructions. At 48 h post-transfection, cells were harvested, infected with IAVÄNS1, and then subjected to Real Time PCR, immunofluorescence assays, or SDS-PAGE followed by immunoblotting.

Fluorescence in situ Hybridization (FISH) Assay

FISH assays have been described previously [57]. Briefly, after the immunofluorescence assays, cells were fixed in 4%PFA for 10 min and permeablized on ice with 0.5% Triton X-100 in PBS for 5 min. After deproteinization by Proteinase K, cells were re-fixed in 4% PFA for 10 min and then subjected to stepwise dehydration in ethanol. The dried coverslips were incubated with a biotin-labeled RNA probe for 12 h at 37°C. After hybridization, cells were washed and incubated with avidin-FITC for 30 min at 37°C. Nuclei were stained with TO-PRO-3 and examined by confocal laser-scanning microscope.

Enzyme-linked Immunosorbent Assay (ELISA)

Culture supernatants were collected and subjected to ELISA with mouse IFN-â kit (PBL Interferon Source) according to the manufacturers' instructions.

Supporting Information

Figure S1 Anti-RIG-I antibody specifically recognizes endogenous human RIG-I. HeLa cells were infected with control lentivirus or two lentiviruses encoding different RIG-I-specific shRNAs (#1 and #2) for 72 h. **(A)** The cells were treated with $NaAsO_2$ for 1 h and stained for RIG-I and G3BP. $NaAsO_2$ induces speckle-like localization of RIG-I and G3BP. **(B)** The cells were treated with human IFN-â for 12 h. Cell extracts were prepared and subjected to SDS-PAGE, and immunoblotted using antibodies against RIG-I, MDA5, and â-actin. The RIG-I signals were diminished by knockdown of RIG-I.
(TIF)

Figure S2 N-terminal region of NS1 is sufficient to block RIG-I aggregation and antiviral signals. **(A)** 293T cells were transfected with empty vector (empty), myc-tagged NS1 (myc-NS1 (Full)), N-terminal NS1 (1–80), or C-terminal NS1 (81–230) for 48 h. The cells were mock-treated (mock) or infected with IAVÄNS1 for 9 h and stained for RIG-I and NS1 (myc). The percentage of cells with IAVÄNS1-induced RIG-I speckle was 0.0%, 2.3%, 43.1%, for NS1, NS1 (1–80), and NS1 (81–230)-expressing cells, respectively. **(B)** 293T cells were transiently transfected with reporter plasmids containing natural IFN-â promoter together with the indicated NS1-expressing vectors. Transfected cells were mock-treated or infected with IAVÄNS1 for 12 h and subjected to the Dual-Luciferase assay. Data are presented as the mean standard ± error of the mean (SEM).
(TIF)

Figure S3 Localization of Viral RNA in IAV-infected cells. **(A and B)** HeLa cells were mock-treated or infected with IAV for 12 h. Viral RNA (vRNA) was detected by the FISH method using an RNA probe complementary to the segment 1 of IAV and NP **(A)** and RIG-I **(B)** were detected using anti-NP and anti-RIG-I antibodies. TO-PRO-3 was used for staining of nuclear DNA (DNA). Viral RNA and NP did not form foci.
(TIF)

Figure S4 IPS-1 was accumulated in close proximity to the RIG-I foci. HeLa cells stably expressing FLAG-tagged IPS-1 were mock-treated or infected with IAV or IAVÄNS1 for 10 h. The cells were stained with anti-FLAG and anti-RIG-I antibodies and DAPI. The merged images of FLAG and RIG-I are enlarged in the bottom panel. The white arrowheads indicate RIG-I/IPS-1 contacts. These contacts were observed in 74.2% and 1.8% of IAVÄNS1- and IAV-infected cells, respectively.
(TIF)

Figure S5 avSG formation is not a consequence of IFN gene activation. **(A)** 293T cells were transfected with empty vector or the expression vector for IPS-1 (HA-IPS-1) for 24 h. Cells were stained for IRF-3, HA-tag and TIAR. Nuclear IRF-3 was observed in almost all of the IPS-1-expressing cells (95.5%), however these cells exhibited little foci of TIAR (3.0%). **(B)** HEC-1B cells deficient for type I IFN receptor were mock-treated, infected with IAVÄNS1 for 9 h, or treated with $NaAsO_2$ for 1 h as indicated. Cells were stained for RIG-I and G3BP. SGs and avSGs were observed in HEC-1B cells (% colocalization 98.4% and 92.9% for IAVÄNS1 and $NaAsO_2$, respectively). The zoomed images correspond to the boxed regions. **(C)** HeLa cells were mock-treated or infected with SINV, EMCV, or Ad12 dl203 for 9 h, fixed, and stained for RIG-I and G3BP as indicated (% colocalization: 99.2%, 98.4%, and 98.2%, respectively). The zoomed images correspond to the boxed regions.
(TIF)

Figure S6 IAV-induced formation of avSGs was inhibited in PKR knockdown cells. **(A–E)** HeLa cells were transfected with control siRNA (N.C) or siRNA targeting three independent parts of human PKR mRNA (#1 3). **(A)** At 48 h after transfection, cells were harvested and PKR and actin were detected by Western blotting. **(B–E)** At 48 h after transfection, cells were mock-treated (open bar) or infected with IAVÄNS1 (filled bar) for 9 h. The level of IFN-â mRNA was determined by qPCR **(B)**. Immunostaining of HeLa cells transfected with control (N.C) or PKR-targeted (PKR) siRNA after mock-treatment or infection with IAVÄNS1 **(C)**. Cells were also examined by staining for foci of RIG-I **(D)**, TIAR **(E)** after 12 h infection. Percentages of cells containing the respective foci are indicated. Data are presented as the mean standard ± error of the mean (SEM).
(TIF)

Figure S7 Total RNA from IAV-infected cells but not uninfected cells induces avSG formation and IFN-â gene activation. **(A and B)** Wild-type MEF were mock-treated (no RNA) or transfected with total RNA extracted from uninfected MEFs (MEF RNA) or from IAV-infected cells for 12 h (IAV infected MEF RNA). The cells were stained for RIG-I and G3BP (% avSG formation 0.0%, 4.0%, and 21.4% for no RNA, MEF RNA, and IAV infected MEF RNA, respectively) **(A)**. The zoomed images correspond to the boxed regions. Endogenous IFN-â mRNA levels were determined by qPCR **(B)**. Data are presented as the mean standard ± error of the mean (SEM).
(TIF)

Acknowledgments

We thank R. Kageyama for making their confocal microscope available for this study, F. Momose and Y. Kikuchi for the anti-IAV NP antibody, and Y. Sokawa for the anti-OAS antibody.

Author Contributions

Conceived and designed the experiments: KO MY TF. Performed the experiments: KO MJ JY RN SM AT AK SO TM. Analyzed the data: KO KN HN MY TF. Contributed reagents/materials/analysis tools: SS. Wrote the paper: KO MY TF.

References

1. Samuel CE (2001) Antiviral actions of interferons. Clin Microbiol Rev 14: 778–809, table of contents.
2. Witte K, Witte E, Sabat R, Wolk K (2010) IL-28A, IL-28B, and IL-29: promising cytokines with type I interferon-like properties. Cytokine Growth Factor Rev 21: 237–251.
3. Gale M Jr, Katze MG (1998) Molecular mechanisms of interferon resistance mediated by viral-directed inhibition of PKR, the interferon-induced protein kinase. Pharmacol Ther 78: 29–46.
4. Rubinstein S, Familletti PC, Pestka S (1981) Convenient assay for interferons. J Virol 37: 755–758.
5. Yoneyama M, Kikuchi M, Natsukawa T, Shinobu N, Imaizumi T, et al. (2004) The RNA helicase RIG-I has an essential function in double-stranded RNA-induced innate antiviral responses. Nat Immunol 5: 730–737.
6. Kato H, Takeuchi O, Sato S, Yoneyama M, Yamamoto M, et al. (2006) Differential roles of MDA5 and RIG-I helicases in the recognition of RNA viruses. Nature 441: 101–105.
7. Yoneyama M, Kikuchi M, Matsumoto K, Imaizumi T, Miyagishi M, et al. (2005) Shared and unique functions of the DExD/H-box helicases RIG-I, MDA5, and LGP2 in antiviral innate immunity. J Immunol 175: 2851–2858.
8. Hornung V, Ellegast J, Kim S, Brzozka K, Jung A, et al. (2006) 5′-Triphosphate RNA is the ligand for RIG-I. Science 314: 994–997.
9. Pichlmair A, Schulz O, Tan CP, Naslund TI, Liljestrom P, et al. (2006) RIG-I-mediated antiviral responses to single-stranded RNA bearing 5′-phosphates. Science 314: 997–1001.
10. Rasmussen SB, Jensen SB, Nielsen C, Quartin E, Kato H, et al. (2009) Herpes simplex virus infection is sensed by both Toll-like receptors and retinoic acid-inducible gene- like receptors, which synergize to induce type I interferon production. J Gen Virol 90: 74–78.
11. Samanta M, Iwakiri D, Kanda T, Imaizumi T, Takada K (2006) EB virus-encoded RNAs are recognized by RIG-I and activate signaling to induce type I IFN. EMBO J 25: 4207–4214.
12. Onoguchi K, Onomoto K, Takamatsu S, Jogi M, Takemura A, et al. (2010) Virus-infection or 5′ppp-RNA activates antiviral signal through redistribution of IPS-1 mediated by MFN1. PLoS Pathog 6: e1001012.
13. Hale BG, Randall RE, Ortin J, Jackson D (2008) The multifunctional NS1 protein of influenza A viruses. J Gen Virol 89: 2359–2376.
14. Portela A, Digard P (2002) The influenza virus nucleoprotein: a multifunctional RNA-binding protein pivotal to virus replication. J Gen Virol 83: 723–734.
15. Buchan JR, Parker R (2009) Eukaryotic stress granules: the ins and outs of translation. Mol Cell 36: 932–941.
16. Hou F, Sun L, Zheng H, Skaug B, Jiang QX, et al. (2011) MAVS Forms Functional Prion-like Aggregates to Activate and Propagate Antiviral Innate Immune Response. Cell 146: 448–461.
17. Xu LG, Wang YY, Han KJ, Li LY, Zhai Z, et al. (2005) VISA is an adapter protein required for virus-triggered IFN-beta signaling. Mol Cell 19: 727–740.
18. Seth RB, Sun L, Ea CK, Chen ZJ (2005) Identification and characterization of MAVS, a mitochondrial antiviral signaling protein that activates NF-kappaB and IRF 3. Cell 122: 669–682.
19. Kawai T, Takahashi K, Sato S, Coban C, Kumar H, et al. (2005) IPS-1, an adaptor triggering RIG-I- and Mda5-mediated type I interferon induction. Nat Immunol 6: 981–988.
20. Meylan E, Curran J, Hofmann K, Moradpour D, Binder M, et al. (2005) Cardif is an adaptor protein in the RIG-I antiviral pathway and is targeted by hepatitis C virus. Nature 437: 1167–1172.
21. Dixit E, Boulant S, Zhang Y, Lee AS, Odendall C, et al. (2010) Peroxisomes are signaling platforms for antiviral innate immunity. Cell 141: 668–681.
22. White JP, Cardenas AM, Marissen WE, Lloyd RE (2007) Inhibition of cytoplasmic mRNA stress granule formation by a viral proteinase. Cell Host Microbe 2: 295–305.
23. Nallagatla SR, Hwang J, Toroney R, Zheng X, Cameron CE, et al. (2007) 5′-triphosphate-dependent activation of PKR by RNAs with short stem-loops. Science 318: 1455–1458.
24. Baum A, Sachidanandam R, Garcia-Sastre A (2010) Preference of RIG-I for short viral RNA molecules in infected cells revealed by next-generation sequencing. Proc Natl Acad Sci U S A 107: 16303–16308.
25. Rehwinkel J, Tan CP, Goubau D, Schulz O, Pichlmair A, et al. (2010) RIG-I detects viral genomic RNA during negative-strand RNA virus infection. Cell 140: 397–408.
26. Yang YL, Reis LF, Pavlovic J, Aguzzi A, Schafer R, et al. (1995) Deficient signaling in mice devoid of double-stranded RNA-dependent protein kinase. EMBO J 14: 6095–6106.
27. Kato H, Takeuchi O, Mikamo-Satoh E, Hirai R, Kawai T, et al. (2008) Length-dependent recognition of double-stranded ribonucleic acids by retinoic acid-inducible gene-I and melanoma differentiation-associated gene 5. J Exp Med 205: 1601–1610.
28. Yoneyama M, Fujita T (2010) Recognition of viral nucleic acids in innate immunity. Rev Med Virol 20: 4–22.
29. Malathi K, Dong B, Gale M Jr, Silverman RH (2007) Small self-RNA generated by RNase L amplifies antiviral innate immunity. Nature 448: 816–819.
30. Berlanga JJ, Ventoso I, Harding HP, Deng J, Ron D, et al. (2006) Antiviral effect of the mammalian translation initiation factor 2alpha kinase GCN2 against RNA viruses. EMBO J 25: 1730–1740.
31. Ouda R, Onomoto K, Takahasi K, Edwards MR, Kato H, et al. (2011) Retinoic acid-inducible gene I-inducible miR-23b inhibits infections by minor group rhinoviruses through down-regulation of the very low density lipoprotein receptor. J Biol Chem 286: 26210–26219.
32. Saito T, Hirai R, Loo YM, Owen D, Johnson CL, et al. (2007) Regulation of innate antiviral defenses through a shared repressor domain in RIG-I and LGP2. Proc Natl Acad Sci U S A 104: 582–587.
33. Kedersha N, Anderson P (2007) Mammalian stress granules and processing bodies. Methods Enzymol 431: 61–81.
34. Diebold SS, Montoya M, Unger H, Alexopoulou L, Roy P, et al. (2003) Viral infection switches non-plasmacytoid dendritic cells into high interferon producers. Nature 424: 324–328.
35. Gilfoy FD, Mason PW (2007) West Nile virus-induced interferon production is mediated by the double-stranded RNA-dependent protein kinase PKR. J Virol 81: 11148–11158.
36. McAllister CS, Samuel CE (2009) The RNA-activated protein kinase enhances the induction of interferon-beta and apoptosis mediated by cytoplasmic RNA sensors. J Biol Chem 284: 1644–1651.
37. Carpentier PA, Williams BR, Miller SD (2007) Distinct roles of protein kinase R and toll-like receptor 3 in the activation of astrocytes by viral stimuli. Glia 55: 239–252.
38. Barry G, Breakwell L, Fragkoudis R, Attarzadeh-Yazdi G, Rodriguez-Andres J, et al. (2009) PKR acts early in infection to suppress Semliki Forest virus production and strongly enhances the type I interferon response. J Gen Virol 90: 1382–1391.

39. Schulz O, Pichlmair A, Rehwinkel J, Rogers NC, Scheuner D, et al. (2010) Protein kinase R contributes to immunity against specific viruses by regulating interferon mRNA integrity. Cell Host Microbe 7: 354–361.
40. Min JY, Li S, Sen GC, Krug RM (2007) A site on the influenza A virus NS1 protein mediates both inhibition of PKR activation and temporal regulation of viral RNA synthesis. Virology 363: 236–243.
41. Khaperskyy DA, Hatchette TF, McCormick C (2011) Influenza A virus inhibits cytoplasmic stress granule formation. FASEB J.
42. Guo Z, Chen LM, Zeng H, Gomez JA, Plowden J, et al. (2007) NS1 protein of influenza A virus inhibits the function of intracytoplasmic pathogen sensor, RIG-I. Am J Respir Cell Mol Biol 36: 263–269.
43. Mibayashi M, Martinez-Sobrido L, Loo YM, Cardenas WB, Gale M Jr, et al. (2007) Inhibition of retinoic acid-inducible gene I-mediated induction of beta interferon by the NS1 protein of influenza A virus. J Virol 81: 514–524.
44. Gack MU, Albrecht RA, Urano T, Inn KS, Huang IC, et al. (2009) Influenza A virus NS1 targets the ubiquitin ligase TRIM25 to evade recognition by the host viral RNA sensor RIG-I. Cell Host Microbe 5: 439–449.
45. Li W, Li Y, Kedersha N, Anderson P, Emara M, et al. (2002) Cell proteins TIA-1 and TIAR interact with the 3′ stem-loop of the West Nile virus complementary minus-strand RNA and facilitate virus replication. J Virol 76: 11989–12000.
46. Iseni F, Garcin D, Nishio M, Kedersha N, Anderson P, et al. (2002) Sendai virus trailer RNA binds TIAR, a cellular protein involved in virus-induced apoptosis. EMBO J 21: 5141–5150.
47. Simpson-Holley M, Kedersha N, Dower K, Rubins KH, Anderson P, et al. (2010) Formation of antiviral cytoplasmic granules during orthopoxvirus infection. J Virol 85: 1581–1593.
48. Yoneyama M, Suhara W, Fukuhara Y, Fukuda M, Nishida E, et al. (1998) Direct triggering of the type I interferon system by virus infection: activation of a transcription factor complex containing IRF-3 and CBP/p300. EMBO J 17: 1087–1095.
49. Daly C, Reich NC (1993) Double-stranded RNA activates novel factors that bind to the interferon-stimulated response element. Mol Cell Biol 13: 3756–3764.
50. Iwamura T, Yoneyama M, Yamaguchi K, Suhara W, Mori W, et al. (2001) Induction of IRF-3/−7 kinase and NF-kappaB in response to double-stranded RNA and virus infection: common and unique pathways. Genes Cells 6: 375–388.
51. Momose F, Kikuchi Y, Komase K, Morikawa Y (2007) Visualization of microtubule-mediated transport of influenza viral progeny ribonucleoprotein. Microbes Infect 9: 1422–1433.
52. Onoguchi K, Yoneyama M, Takemura A, Akira S, Taniguchi T, et al. (2007) Viral infections activate types I and III interferon genes through a common mechanism. J Biol Chem 282: 7576–7581.
53. Brummelkamp TR, Bernards R, Agami R (2002) A system for stable expression of short interfering RNAs in mammalian cells. Science 296: 550–553.
54. Naldini L, Blomer U, Gallay P, Ory D, Mulligan R, et al. (1996) In vivo gene delivery and stable transduction of nondividing cells by a lentiviral vector. Science 272: 263–267.
55. Zufferey R, Nagy D, Mandel RJ, Naldini L, Trono D (1997) Multiply attenuated lentiviral vector achieves efficient gene delivery in vivo. Nat Biotechnol 15: 871–875.
56. Bridge AJ, Pebernard S, Ducraux A, Nicoulaz AL, Iggo R (2003) Induction of an interferon response by RNAi vectors in mammalian cells. Nat Genet 34: 263–264.
57. Jo S, Kawaguchi A, Takizawa N, Morikawa Y, Momose F, et al. (2010) Involvement of vesicular trafficking system in membrane targeting of the progeny influenza virus genome. Microbes Infect 12: 1079–1084.

Virus Genes (2012) 44:374–381
DOI 10.1007/s11262-012-0712-2

Development of a drug assay system with hepatitis C virus genome derived from a patient with acute hepatitis C

Kyoko Mori · Youki Ueda · Yasuo Ariumi · Hiromichi Dansako · Masanori Ikeda · Nobuyuki Kato

Received: 5 October 2011 / Accepted: 1 January 2012 / Published online: 18 January 2012

Abstract We developed a new cell culture drug assay system (AH1R), in which genome-length hepatitis C virus (HCV) RNA (AH1 strain of genotype 1b derived from a patient with acute hepatitis C) efficiently replicates. By comparing the AH1R system with the OR6 assay system that we developed previously (O strain of genotype 1b derived from an HCV-positive blood donor), we demonstrated that the anti-HCV profiles of reagents including interferon-γ and cyclosporine A significantly differed between these assay systems. Furthermore, we found unexpectedly that rolipram, an anti-inflammatory drug, showed anti-HCV activity in the AH1R assay but not in the OR6 assay, suggesting that the anti-HCV activity of rolipram differs depending on the HCV strain. Taken together, these results suggest that the AH1R assay system is useful for the objective evaluation of anti-HCV reagents and for the discovery of different classes of anti-HCV reagents.

Keywords HCV · Acute hepatitis C · Anti-HCV drug assay system · Anti-HCV activity of rolipram

Introduction

Hepatitis C virus (HCV) infection frequently causes chronic hepatitis, which progresses to liver cirrhosis and hepatocellular carcinoma. HCV is an enveloped virus with a positive single-stranded 9.6 kb RNA genome, which encodes a large polyprotein precursor of approximately 3,000 amino acid (aa) residues [1, 2]. This polyprotein is cleaved by a combination of the host and viral proteases into at least 10 proteins in the following order: Core, envelope 1 (E1), E2, p7, non-structural 2 (NS2), NS3, NS4A, NS4B, NS5A, and NS5B [1].

Human hepatoma HuH-7 cell culture-based HCV replicon systems derived from a number of HCV strains have been widely used for various studies on HCV RNA replication [3, 4] since the first replicon system (based on the Con1 strain of genotype 1b) was developed in 1999 [5]. Genome-length HCV RNA replication systems (see Fig. 2 for details) derived from a limited number of HCV strains (H77, N, Con1, O, and JFH-1) are also sometimes used for such studies, as they are more useful than the replicon systems lacking the structural region of HCV, although the production of infectious HCV from the genome-length HCV RNA has not been demonstrated to date [3, 4]. Furthermore, these RNA replication systems have been improved enough to be suitable for the screening of anti-HCV reagents by the introduction of reporter genes such as luciferase [3, 4, 6]. We also developed an HuH-7-derived cell culture assay system (OR6) in which genome-length HCV RNA (O strain of genotype 1b derived from an HCV-positive blood donor) encoding renilla luciferase (RL) efficiently replicates [7]. Such reporter assay systems could save time and facilitate the mass screening of anti-HCV reagents, since the values of luciferase correlated well with the level of HCV RNA after treatment with anti-HCV reagents. Furthermore, OR6 assay system became more useful as a drug assay system than the HCV subgenomic replicon-based reporter assay systems developed to date [3, 4], because the older systems lack the Core-NS2 regions containing structural proteins likely to be involved in the events that take place in the HCV-infected human liver.

K. Mori · Y. Ueda · Y. Ariumi · H. Dansako · M. Ikeda · N. Kato (✉)
Department of Tumor Virology, Okayama University Graduate School of Medicine, Dentistry, and Pharmaceutical Sciences, 2-5-1 Shikata-cho, Okayama 700-8558, Japan
e-mail: nkato@md.okayama-u.ac.jp

Indeed, by the screening of preexisting drugs using the OR6 assay system, we have identified mizoribine [8], statins [9], hydroxyurea [10], and teprenone [11] as new anti-HCV drug candidates, indicating that the OR6 assay system is useful for the discovery of anti-HCV reagents.

On the other hand, we previously established for the first time an HuH-7-derived cell line (AH1) that harbors genome-length HCV RNA (AH1 strain of genotype 1b) derived from a patient with acute hepatitis C [12]. In that study, we noticed different anti-HCV profiles of interferon (IFN)-γ or cyclosporine A (CsA) between AH1 and O cells supporting genome-length HCV RNA (O strain) replication [7]. From these results, we supposed that the diverse effects of IFN-γ or CsA were attributable to the difference in HCV strains [12].

To test this assumption in detail, we first developed an AH1 strain-derived assay system (AH1R) corresponding to the OR6 assay system, and then performed a comparative analysis using AH1R and OR6 assay systems. In this article, we report that the difference in HCV strains causes the diverse effects of anti-HCV reagents, and we found unexpectedly by AH1R assay that rolipram, an anti-inflammatory drug, is an anti-HCV drug candidate.

Materials and methods

Reagents

IFN-α, IFN-γ, and CsA were purchased from Sigma-Aldrich (St. Louis, MO). Rolipram was purchased from Wako Pure Chemical Industries (Osaka, Japan).

Plasmid construction

The plasmid pAH1RN/C-5B/PL,LS,TA,$(VA)_3$ was constructed from pAH1 N/C-5B/PL,LS,TA,$(VA)_3$ encoding genome-length HCV RNA clone 2 (See Fig. 2) obtained from AH1 cells [12], by introducing a fragment of the RL gene from pORN/C-5B into the *Asc*I site before the neomycin phosphotransferase (Neo^R) gene as previously described [7].

RNA synthesis

The plasmid pAH1RN/C-5B/PL,LS,TA,$(VA)_3$ DNA was linearized by *Xba*I, and used for RNA synthesis with T7 MEGAscript (Ambion, Austin TX) as previously described [7].

Cell cultures

AH1R and OR6 cells supporting genome-length HCV RNAs were cultured in Dulbecco's modified Eagle's medium (DMEM) supplemented with 10% fetal bovine serum (FBS) and 0.3 mg/mL of G418 (Geneticin; Invitrogen, Carlsbad, CA). AH1c-cured cells, which were created by eliminating HCV RNA from AH1 cells [12] by IFN-γ treatment, were also cultured in DMEM supplemented with 10% FBS.

RNA transfection and selection of G418-resistant cells

Genome-length HCV (AH1RN/C-5B/PL,LS,TA,$(VA)_3$) RNA synthesized in vitro was transfected into AH1c cells by electroporation, and the cells were selected in the presence of G418 (0.3 mg/mL) for 3 weeks as described previously [13].

RL assay for anti-HCV reagents

To monitor the effects of anti-HCV reagents, RL assay was performed as described previously [14]. Briefly, the cells were plated onto 24-well plates (2×10^4 cells per well) in triplicate and cultured with the medium in the absence of G418 for 24 h. The cells were then treated with each reagent at several concentrations for 72 h. After treatment, the cells were subjected to a luciferase assay using the RL assay system (Promega, Madison, WI). From the assay results, the 50% effective concentration (EC_{50}) of each reagent was determined.

Quantification of HCV RNA

Quantitative reverse transcription-polymerase chain reaction (RT-PCR) analysis for HCV RNA was performed using a real-time LightCycler PCR (Roche Applied Science, Indianapolis, IN, USA) as described previously [7]. The experiments were done in triplicate.

IFN-α treatment to evaluate the assay systems

To monitor the anti-HCV effect of IFN-α on AH1R cells, 2×10^4 cells and 5×10^5 cells were plated onto 24-well plates (for luciferase assay) and 10 cm plates (for quantitative RT-PCR assay) in triplicate, respectively, and cultured for 24 h. The cells were then treated with IFN-α at final concentrations of 0, 1, 10, and 100 IU/mL for 24 h, and subjected to luciferase and quantitative RT-PCR assays as described above.

Western blot analysis

The preparation of cell lysates, sodium dodecyl sulfate–polyacrylamide gel electrophoresis, and immunoblotting analysis with a PVDF membrane were performed as described previously [13]. The antibodies used in this study were those against HCV Core (CP11 monoclonal antibody;

Institute of Immunology, Tokyo), NS5B, and E2 (generous gifts from Dr. M. Kohara, Tokyo Metropolitan Institute of Medical Science, Japan). Anti-β-actin antibody (AC-15; Sigma, St. Louis, MO, USA) was used as a control for the amount of protein loaded per lane. Immunocomplexes were detected with the Renaissance enhanced chemiluminescence assay (Perkin-Elmer Life Sciences, Boston, MA).

WST-1 cell proliferation assay

The cells were plated onto 96-well plates (1×10^3 cells per well) in triplicate and then treated with rolipram at several concentrations for 72 h. After treatment, the cells were subjected to the WST-1 cell proliferation assay (Takara Bio, Otsu, Japan) according to the manufacturer's protocol. From the assay results, the 50% cytotoxic concentration (CC_{50}) of rolipram was estimated. The selective index (SI) value of rolipram was also estimated by dividing the CC_{50} value by the EC_{50} value.

RT-PCR and sequencing

To amplify the genome-length HCV RNA, RT-PCR was performed separately in two fragments as described previously [7, 15]. Briefly, one fragment covered from 5′-untranslated region to NS3, with a final product of approximately 6.2 kb, and the other fragment covered from NS2 to NS5B, with a final product of approximately 6.1 kb. These fragments overlapped at the NS2 and NS3 regions and were used for sequence analysis of the HCV open reading frame (ORF) after cloning into pBR322MC. PrimScript (Takara Bio) and KOD-plus DNA polymerase (Toyobo, Osaka, Japan) were used for RT and PCR, respectively. The nucleotide sequences of each of the three independent clones obtained were determined using the Big Dye terminator cycle sequencing kit on an ABI PRISM 310 genetic analyzer (Applied Biosystems, Foster City, CA, USA).

Statistical analysis

Differences between AH1R and OR6 cell lines were tested using Student's t test. P values <0.05 were considered statistically significant.

Results

Development of a luciferase reporter assay system that facilitates the quantitative monitoring of genome-length HCV-AH1 RNA replication

To develop an HCV AH1 strain-derived assay system corresponding to the OR6 assay system [7], a genome-length HCV RNA encoding RL (AH1RN/C-5B/PL,LS,TA,$(VA)_3$) was transfected into AH1c cells. Following 3 weeks of culturing in the presence of G418, more than 10 colonies were obtained, and then 8 colonies (#2, #3, #4, #5, #6, #8, #13, and #14) were successfully proliferated. We initially selected colonies #2, #3, and #14 because they had high levels of RL activity ($>4 \times 10^6$ U/1.6×10^5 cells) (Fig. 1a). However, RT-PCR and the sequencing analyses revealed that the genome-length HCV-AH1 RNAs obtained from these colonies each had an approximately 1 kb deletion in the E2 region (data not shown). In this regard, we previously observed similar phenomenon and described the difficulty of the development of a luciferase reporter assay system using the genome-length HCV RNA of more than 12 kb [7], suggesting that the NS5B polymerase possesses the limited elongation ability (probably up to a total length of 12 kb). Indeed, in that study, we could overcome this obstacle by the selection of the colony harboring a complete genome-length HCV RNA among the obtained G418-resistant colonies [7]. Therefore, we next carried out the selection among the other colonies. Fortunately, we found that colony #4, showing a rather high level of RL activity (2×10^6 U/1.6×10^5 cells), possessed a complete genome-length HCV-AH1 RNA without any deleted forms, although most of the other colonies possessed some amounts of a deleted form in addition to a complete genome-length HCV-AH1 RNA (data not shown). We demonstrated that the HCV RNA sequence was not integrated into the genomic DNA in colony #4 (data not shown). From these results, we finally selected colony #4, and it was thereafter referred to as AH1R and used for the following studies.

We first demonstrated that AH1R cells expressed sufficient levels of HCV proteins (Core, E2, and NS5B) by Western blot analysis for the evaluation of anti-HCV reagents, and the expression levels were almost equivalent to those in OR6 cells (Fig. 1b). In this analysis, we confirmed that the size of the E2 protein in AH1R cells was 7 kDa larger than that in OR6 cells (Fig. 1b), as observed previously [12]. This result indicates that AH1R cells express AH1 strain-derived E2 protein possessing two extra N-glycosylation sites [12]. We next demonstrated good correlations between the levels of RL activity and HCV RNA in AH1R cells (Fig. 1c), as we previously demonstrated in OR6 cells treated with IFN-α for 24 h [7]. These correlations indicate that AH1R cells were as useful as OR6 cells as a luciferase assay system.

Aa substitutions detected in genome-length HCV RNA in AH1R cells

To examine whether or not genome-length HCV RNA in AH1R cells possesses additional conserved mutations such as adaptive mutations, we performed a sequence analysis of HCV RNA in AH1R cells. The results (Fig. 2) revealed that

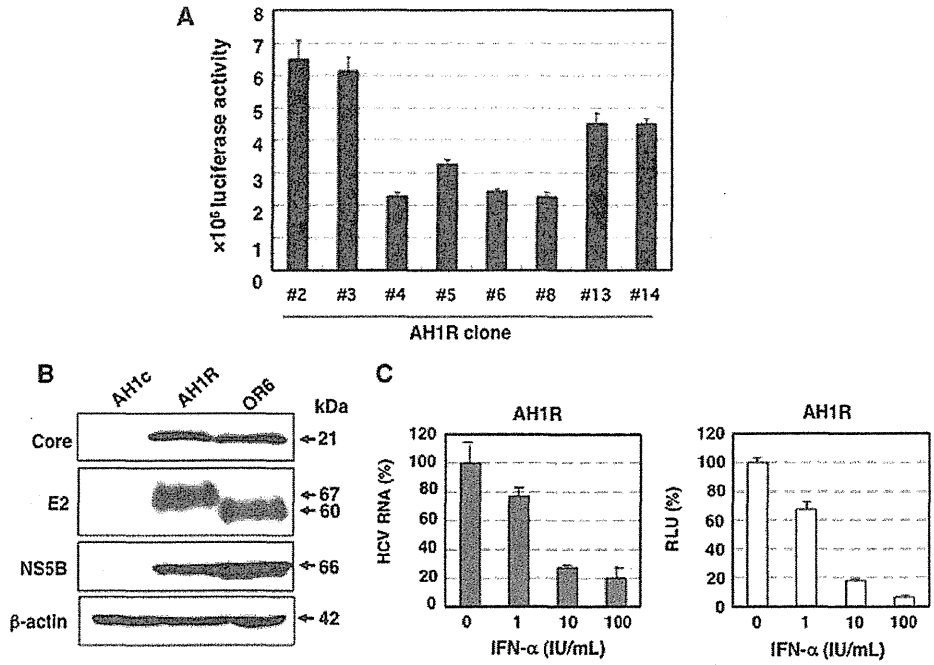

Fig. 1 Characterization of AH1R cells harboring genome-length HCV RNA. **a** Selection of G418-resistant cell clones. The levels of HCV RNA in G418-resistant cells were monitored by RL assay. **b** Western blot analysis. AH1c, AH1R, and OR6 cells were used for the comparison. *Core, E2,* and *NS5B* were detected by Western blot analysis. β-actin was used as a control for the amount of protein loaded per lane. **c** RL activity is correlated with HCV RNA level. The AH1R cells were treated with IFN-α (0, 1, 10, and 100 IU/mL) for 24 h, and then a luciferase reporter assay (*right panel*) and quantitative RT-PCR (*left panel*) were performed. The relative luciferase activity (RLU) (%) or HCV RNA (%) calculated at each point, when the level of luciferase activity or HCV RNA in non-treated cells was assigned to be 100%, is presented here

two additional mutations accompanying aa substitutions (W860R (NS2) and A1218E (NS3)) were detected commonly among the three independent clones sequenced, suggesting that these additional mutations are required for the efficient replication or stability of genome-length HCV RNA. The P1115L (NS3), L1262S (NS3), V1897A (NS4B), and V2360A (NS5A) mutations derived from the sAH1 replicon [12] were conserved in AH1R cell-derived clones. However, AH1-clone-2-specific mutations (T1338A and V1880A) were almost reverted to the consensus sequences of AH1 RNA [12] except for V1880A in AH1R clone 2 (Fig. 2). In addition, the Q63R (Core) mutation was observed in two of three clones (Fig. 2).

Comparison between the AH1R and OR6 assay systems regarding the sensitivities to IFN-α, IFN-γ, and CsA

Using quantitative RT-PCR analysis, we previously examined the anti-HCV activities of IFN-α, IFN-γ, and CsA in AH1 and O cells, and noticed different anti-HCV profiles of IFN-γ and CsA between AH1 and O cells [12]. In that study, AH1 cells seemed to be more sensitive than the O cells to CsA (significant difference was observed when 0.063, 0.12, or 0.25 μg/mL of CsA was used). Conversely, AH1 cells seemed to be less sensitive than the O cells to IFN-γ (significant difference was observed when 1 or 10 IU/mL of IFN-γ was used). However, we were not able to determine precisely the EC_{50} values of these reagents, because of the unevenness of the data obtained by RT-PCR.

After developing the AH1R assay system in this study, we determined the EC_{50} values of IFN-α, IFN-γ, and CsA using the AH1R assay and compared the values with those obtained by the OR6 assay. The results revealed that AH1R assay was more sensitive than OR6 assay to IFN-α (EC_{50}; 0.31 IU/mL for AH1R, 0.45 IU/mL for OR6) (Fig. 3a) and CsA (EC_{50}; 0.11 μg/mL for AH1R, 0.42 μg/mL for OR6) (Fig. 3b), and that the OR6 assay was more sensitive than the AH1R assay to IFN-γ (EC_{50}; 0.69 IU/mL for AH1R, 0.28 IU/mL for OR6) (Fig. 3c). Regarding these anti-HCV reagents, the anti-HCV activities observed between the AH1R and OR6 assays differed significantly in all of the concentrations examined (Fig. 3). In addition, regarding these anti-HCV reagents, cell growth was not suppressed within the concentrations used. Regarding IFN-γ and CsA, the present results clearly support those of our previous

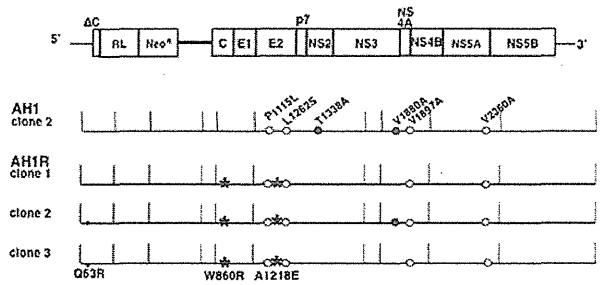

Fig. 2 Aa substitutions detected in intracellular AH1R genome-length HCV RNA. The *upper portion* shows schematic gene organization of genome-length HCV RNA encoding the *RL* gene developed in this study. Genome-length HCV RNA consists of 2 cistrons. In the first cistron, RL is translated as a fusion protein with Neo^R by HCV-IRES, and in the second cistron, all of HCV proteins (C-NS5B) are translated by encephalomyocarditis virus (EMCV)-IRES introduced in the region upstream of C-NS5B regions. Genome-length HCV RNA-replicating cells possess the G418-resistant phenotype because Neo^R is produced by the efficient replication of genome-length HCV RNA. Therefore, when genome-length HCV RNA is excluded from the cells or when its level is decreased, the cells are killed in the presence of G418. In this system, anti-HCV activity is able to evaluate the value of the reporter (RL activity) instead of the quantification of HCV RNA or HCV proteins. In addition, it has been known that the infectious HCV is not produced from this RNA replication system [3, 4, 6]. Core to NS5B regions of three independent clones (*AH1R clones 1–3*) sequenced are presented. W860R and A1218E conserved substitutions are indicated by *asterisks*. Q63R substitutions detected in two of three clones are each indicated by a *small dot*. Core to NS5B regions of *AH1 clone 2*, used to establish the AH1R cell line, are also presented. AH1-specific conserved substitutions and *AH1-clone-2*-specific substitutions are indicated by *open circles* and *black circles*, respectively

study [12]. Therefore, we suggest that the diverse effects of these anti-HCV reagents are due to the difference in HCV strains, although we are not able to completely exclude the possibility that AH1R cells are compromised cells causing the different responses against anti-HCV reagents. In summary, the previous and present findings suggest that the AH1R assay system is also useful for the evaluation of anti-HCV reagents as an independent assay system.

Anti-HCV activity of rolipram was clearly observed in the AH1R assay, but not in the OR6 assay

From the above findings, we supposed that the anti-HCV reagents reported to date might show diverse effects between the drug assay systems derived from the different HCV strains. To test this assumption, we used the AH1R and OR6 assay systems to evaluate the anti-HCV activity of more than 10 pre-existing drugs (6-Azauridine, bisindoly maleimide 1, carvedilol, cehalotaxine, clemizole, 2′-deoxy-5-fluorouridine, esomeprazole, guanazole, hemin, homoharringtonine, methotrexate, nitazoxanide, resveratrol, rolipram, silibinin A, Y27632, etc.), which other groups had evaluated using an assay system derived from the Con1 strain (genotype 1b) or JFH-1 strain (genotype 2a). The results revealed that most of these reagents in the AH1R assay showed similar levels of anti-HCV activities compared with those in the OR6 assay or those of the previous studies (data not shown). However, we found that only rolipram, a selective phosphodiesterase 4 (PDE4) inhibitor [16] that is used as an anti-inflammatory drug, showed moderate anti-HCV activity (EC_{50} 31 μM; $CC_{50} > 200$ μM; $SI > 6$) in the AH1R assay, but no such activity in the OR6 assay (upper panel in Fig. 4a). This remarkable difference was confirmed by Western blot analysis (lower panel in Fig. 4a). It is unlikely that rolipram's anti-HCV activity is due to the inhibition of exogenous RL, Neo^R or encephalomyocarditis virus internal ribosomal entry site (EMCV-IRES), all of which are encoded in the genome-length HCV RNA, because the AH1R and OR6 assay systems possess the same structure of genome-length HCV RNA except for HCV ORF. To demonstrate that rolipram's anti-HCV activity is not due to the clonal specificity of the cells or the specificity of genome-length HCV RNA, we examined the anti-HCV activity of rolipram using the monoclonal HCV replicon RNA-replicating cells (sAH1 cells for AH1 strain [12], and sO cells for O strain [13]). The results

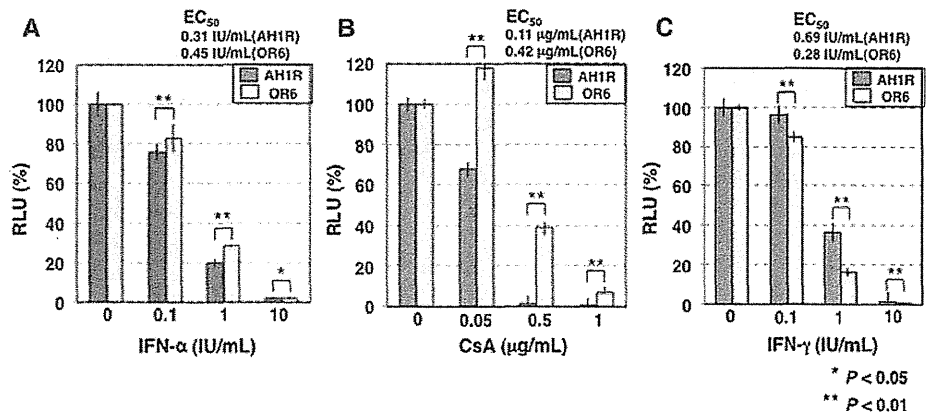

Fig. 3 The diverse effects of anti-HCV reagents on AH1R and OR6 assay systems. AH1R and OR6 cells were treated with anti-HCV reagents for 72 h, and then the RL assay was performed as described in Fig. 1c. **a** Effect of IFN-α. **b** Effect of CsA. **c** Effect of IFN-γ

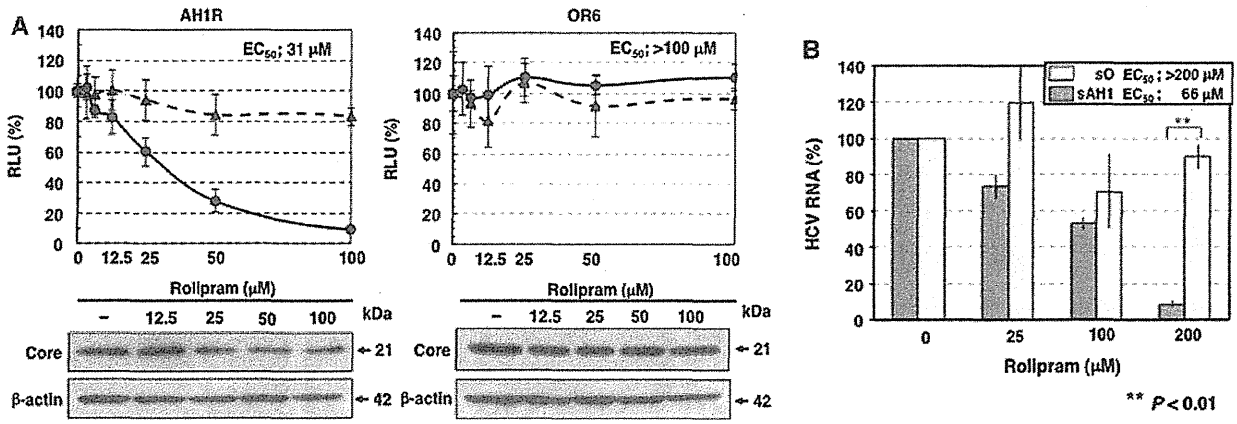

Fig. 4 Anti-HCV activity of rolipram. **a** Rolipram sensitivities on genome-length HCV RNA replication in AH1R and OR6 assay systems. AH1R and OR6 cells were treated with rolipram for 72 h, followed by RL assay (*black circle* with *linear line* in the *upper panels*) and WST-1 assay (*black triangle* with *broken line* in the *upper panels*). The relative value (%) calculated at each point, when the level in non-treated cells was assigned to 100%, is presented here. Western blot analysis of the treated cells for the HCV Core was also performed (*lower panels*). **b** Rolipram sensitivities on HCV replicon RNA replication in sAH1 and sO cells. sAH1 and sO cells were treated with rolipram for 72 h, and extracted total RNAs were subjected to quantitative RT-PCR for HCV 5′ untranslated region as described previously [7]. The HCV RNA (%) calculated at each point, when the level of HCV RNA in non-treated cells was assigned to be 100%, is presented here

revealed by quantitative RT-PCR that rolipram showed moderate anti-HCV activity (EC_{50} 66 μM) in sAH1 cells, but no such activity in sO cells (Fig. 4b). Anti-HCV activity of rolipram in sAH1 cells was a little weaker than that in AH1R cells (Fig. 4b). The similar phenomenon that the anti-HCV activity in genome-length HCV RNA-based reporter assay is stronger than that in HCV subgenomic replicon-based reporter assay was observed regarding other anti-HCV reagents in our previous studies [14, 17, 18]. This result suggests that the anti-HCV activity of rolipram is not either a clone-specific or genome-length HCV RNA-specific phenomenon. In our previous studies also [14, 18], we demonstrated that anti-HCV activities of several reagents including ribavirin and statins were not due to the clonal specificity of the cells. On the other hand, it was recently reported that rolipram did not show anti-HCV activity in the JFH-1 strain-derived assay [19]. Taken together, the previous and present results suggest that rolipram's anti-HCV activity differs depending on the HCV strain. In summary, rolipram was identified as a new anti-HCV candidate using the AH1R assay system.

Discussion

In the present study, we developed for the first time a drug assay system (AH1R), derived from the HCV-AH1 strain (from a patient with acute hepatitis C), in which HCV-AH1 RNA is efficiently replicated. Using this system, we found that rolipram, an anti-inflammatory drug, had potential anti-HCV activity. This potential had not been detected by preexisting assay systems such as OR6, in which HCV-O RNA was derived from an HCV-positive blood donor. Since an HCV replicon harboring the sAH1 cell line, the parent of the AH1R cell line, was obtained from OR6-cured cells [12], the divergence in rolipram's effects between AH1R and OR6 cells is probably attributable to the difference in HCV strains rather than to the difference in cell clones. Indeed, rolipram's anti-HCV activity was not observed in another ORL8 assay system (O strain), which was recently developed using a new hepatoma Li23 cell line (data not shown) [15]. Therefore, we propose that multiple assay systems derived from different HCV strains are required for the discovery of anti-HCV reagents such as rolipram or for the objective evaluation of anti-HCV activity.

Comparative evaluation analysis of anti-HCV activities of IFN-α, IFN-γ, and CsA using AH1-strain-derived AH1R and O-strain-derived OR6 assay systems demonstrated that each of these anti-HCV reagents showed significantly diverse antiviral effects between the two systems. Regarding IFN-γ and CsA, the present results obtained using a luciferase reporter assay fully supported our previous findings [12] using quantitative RT-PCR analysis. However, in the present analysis, we noticed that IFN-α also showed significantly diverse effects (especially at less than 1 IU/mL) between the AH1R and OR6 assays.

The differences in IFN-α sensitivity may be attributable to the difference in aa sequences in the IFN sensitivity-determining region (ISDR; aa 2209-2248 in the HCV-1b genotype), in which aa substitutions correlate well with IFN sensitivity in patients with chronic hepatitis C [20], because the AH1 strain possesses three aa substitutions (T2217A, H2218R, and A2224 V) in ISDR, whereas the O strain possesses no aa substitutions. However, no report has demonstrated the correlation between IFN sensitivity and the substitution numbers in ISDR using the cell culture-based HCV RNA replication system.

Alternatively, Akuta et al. [21] reported that aa substitutions at position 70 and/or position 91 in the HCV Core region of patients infected with the HCV-1b genotype are pretreatment predictors of null virological response (NVR) to pegylated IFN/ribavirin combination therapy. In particular, substitutions of arginine (R) by glutamine (Q) at position 70, and/or leucine (L) by methionine (M) at position 91, were common in NVR. The patients with position-70 substitutions often showed little or no decrease in HCV RNA levels during the early phase of IFN-α treatment [21]. Regarding this point, it is interesting that position 70 in the AH1 strain is R (wild type) and that in the O strain is Q (mutant type), whereas position 91 is L (wild type) in both strains. Therefore, wild-type R in position 70 of the AH1 strain may contribute to the high sensitivity to IFN-α in the AH1R assay. Regarding positions 70 and 91 of the HCV Core, it is noteworthy that, among all of the HCV strains used thus far to develop HCV replicon systems, only the AH1 strain possesses double wild-type aa (data not shown). Therefore, the AH1R assay system may be useful for further study of sensitivity to IFN/ribavirin treatment.

The anti-HCV activity of rolipram, which is currently used as an anti-inflammatory drug, is interesting, although its anti-HCV mechanism is unclear. As a selective PDE4 inhibitor [16], rolipram may attenuate fibroblast activities that can lead to fibrosis and may be particularly effective in the presence of transforming growth factor (TGF)-β1-induced fibroblast stimulation [22]. On the other hand, HCV enhances hepatic fibrosis progression through the generation of reactive oxygen species and the induction of TGF-β1 [23]. Taken together, the previous and present results suggest that rolipram may inhibit both HCV RNA replication and HCV-enhanced hepatic fibrosis. However, it is unclear that rolipram shows anti-HCV activity against the majority of HCV strains, because rolipram has been effective for AH1 strain, but not for O strain. Although rolipram's anti-HCV activity would be HCV-strain-specific, it is not clear which HCV strain is the major type regarding the sensitivity to rolipram. Since developed assay systems using genome-length HCV RNA-replicating cells are limited to several HCV strains including O and AH1 strains to date, further analysis using the assay systems of other HCV strains will be needed to clarify this point.

In this study, we demonstrated that the AH1R assay system, which was for the first time developed using an HCV strain derived from a patient with acute hepatitis C, showed different sensitivities against anti-HCV reagents in comparison with assay systems in current use, such as OR6 assay. Therefore, AH1R assay system would be useful for various HCV studies including the evaluation of anti-HCV reagents and the identification of antiviral targets.

Acknowledgment This study was supported by grants-in-aid for research on hepatitis from the Ministry of Health, Labor, and Welfare of Japan. K. M. was supported by a Research Fellowship for Young Scientists from the Japan Society for the Promotion of Science.

References

1. N. Kato, Acta Med. Okayama **55**, 133–159 (2001)
2. N. Kato, M. Hijikata, Y. Ootsuyama, M. Nakagawa, S. Ohkoshi, T. Sugimura, K. Shimotohno, Proc. Natl. Acad. Sci. USA **87**, 9524–9528 (1990)
3. R. Bartenschlager, S. Sparacio, Virus Res. **127**, 195–207 (2007)
4. D. Moradpour, F. Penin, C.M. Rice, Nat. Rev. Microbiol. **5**, 453–463 (2007)
5. V. Lohmann, F. Korner, J. Koch, U. Herian, L. Theilmann, R. Bartenschlager, Science **285**, 110–113 (1999)
6. M. Ikeda, N. Kato, Adv. Drug Deliv. Rev. **59**, 1277–1289 (2007)
7. M. Ikeda, K. Abe, H. Dansako, T. Nakamura, K. Naka, N. Kato, Biochem. Biophys. Res. Commun. **329**, 1350–1359 (2005)
8. K. Naka, M. Ikeda, K. Abe, H. Dansako, N. Kato, Biochem. Biophys. Res. Commun. **330**, 871–879 (2005)
9. M. Ikeda, K. Abe, M. Yamada, H. Dansako, K. Naka, N. Kato, Hepatology **44**, 117–125 (2006)
10. A. Nozaki, M. Morimoto, M. Kondo, T. Oshima, K. Numata, S. Fujisawa, T. Kaneko, E. Miyajima, S. Morita, K. Mori, M. Ikeda, N. Kato, K. Tanaka, Arch. Virol. **155**, 601–605 (2010)
11. M. Ikeda, Y. Kawai, K. Mori, M. Yano, K. Abe, G. Nishimura, H. Dansako, Y. Ariumi, T. Wakita, K. Yamamoto, N. Kato, Liver Int. **31**, 871–880 (2011)
12. K. Mori, K. Abe, H. Dansako, Y. Ariumi, M. Ikeda, N. Kato, Biochem. Biophys. Res. Commun. **371**, 104–109 (2008)
13. N. Kato, K. Sugiyama, K. Namba, H. Dansako, T. Nakamura, M. Takami, K. Naka, A. Nozaki, K. Shimotohno, Biochem. Biophys. Res. Commun. **306**, 756–766 (2003)
14. K. Mori, M. Ikeda, Y. Ariumi, H. Dansako, T. Wakita, N. Kato, Virus Res. **157**, 61–70 (2011)
15. N. Kato, K. Mori, K. Abe, H. Dansako, M. Kuroki, Y. Ariumi, T. Wakita, M. Ikeda, Virus Res. **146**, 41–50 (2009)
16. S.J. MacKenzie, M.D. Houslay, Biochem. J. **347**, 571–578 (2000)
17. M. Yano, M. Ikeda, K. Abe, H. Dansako, S. Ohkoshi, Y. Aoyagi, N. Kato, Antimicrob. Agents Chemother. **51**, 2016–2027 (2007)
18. G. Nishimura, M. Ikeda, K. Mori, T. Nakazawa, Y. Ariumi, H. Dansako, N. Kato, Antiviral Res. **82**, 42–50 (2009)
19. P. Gastaminza, C. Whitten-Baue, F.V. Chisari, Proc. Natl. Acad. Sci. USA **107**, 291–296 (2010)
20. N. Enomoto, I. Sakuma, Y. Asahina, M. Kurosaki, T. Murakami, C. Yamamoto, Y. Ogura, N. Izumi, F. Marumo, C. Sato, N. Engl. J. Med. **334**, 77–81 (1996)

21. N. Akuta, F. Suzuki, Y. Kawamura, H. Yatsuji, H. Sezaki, Y. Suzuki, T. Hosaka, M. Kobayashi, M. Kobayashi, Y. Arase, K. Ikeda, H. Kumada, J. Med. Virol. **79**, 1686–1695 (2007)
22. S. Togo, X. Liu, X. Wang, Am. J. Physiol. Lung Cell. Mol. Physiol. **296**, L959–L969 (2009)
23. W. Lin, W.L. Tsai, R.X. Shao, G. Wu, L.F. Peng, L.L. Barlow, W.J. Chung, L. Zhang, H. Zhao, J.Y. Jang, R.T. Chung, Gastroenterology **138**, 2509–2518 (2010)

Journal of General Virology (2012), 93, 1422–1431 DOI 10.1099/vir.0.040725-0

Development of hepatitis C virus production reporter-assay systems using two different hepatoma cell lines

Midori Takeda,[1] Masanori Ikeda,[1] Yasuo Ariumi,[1]† Takaji Wakita[2] and Nobuyuki Kato[1]

Correspondence
Masanori Ikeda
maikeda@md.okayama-u.ac.jp

[1]Department of Tumor Virology, Okayama University, Graduate School of Medicine, Dentistry and Pharmaceutical Sciences, Okayama 700-8544, Japan

[2]Department of Virology II, National Institute of Infectious Disease, Tokyo 162-8640, Japan

A hepatitis C virus (HCV) infection system was developed previously using the HCV JFH-1 strain (genotype 2a) and HuH-7 cells, and this cell culture is so far the only robust production system for HCV. In patients with chronic hepatitis C, the virological effects of pegylated interferon and ribavirin therapy differ depending on the HCV strain and the genetic background of the host. Recently, we reported the hepatoma-derived Li23 cell line, in which the JFH-1 life cycle is reproduced at a level almost equal to that in HuH-7-derived RSc cells. To monitor the HCV life cycle more easily, we here developed JFH-1 reporter-assay systems using both HuH-7- and Li23-derived cell lines. To identify any genetic mutations by long-term cell culture, HCV RNAs in HuH-7 cells were amplified 130 days after infection and subjected to sequence analysis to find adaptive mutation(s) for robust virus replication. We identified two mutations, H2505Q and V2995L, in the NS5B region. V2995L but not H2505Q enhanced JFH-1 RNA replication. However, we found that H2505Q but not V2995L enhanced HCV RNA replication of strain O (genotype 1b). We also selected highly permissive D7 cells by serial subcloning of Li23 cells. The expression levels of claudin-1 and Niemann–Pick C1-like 1 in D7 cells are higher than those in parental Li23 cells. In this study, we developed HCV JFH-1 reporter-assay systems using two distinct hepatoma cell lines, HuH-7 and Li23. The mutations in NS5B resulted in different effects on strains O and JFH-1 HCV RNA replication.

Received 21 December 2011
Accepted 26 March 2012

INTRODUCTION

Hepatitis C virus (HCV) infection frequently causes chronic hepatitis and leads to liver cirrhosis and hepatocellular carcinoma. Elimination of HCV by antiviral reagents seems to be the most efficient therapy to prevent fatality.

HCV belongs to the family *Flaviviridae* and contains a positive ssRNA genome of 9.6 kb. The HCV genome encodes a single polyprotein precursor of approximately 3000 aa, which is cleaved by host and viral proteases into at least 10 proteins in the following order: Core, envelope 1 (E1), E2, p7, non-structural 2 (NS2), NS3, NS4A, NS4B, NS5A and NS5B (Kato, 2001; Kato *et al.*, 1990; Tanaka *et al.*, 1996).

Evaluation of anti-HCV reagents was difficult before the development of the HCV replicon system (Lohmann *et al.*, 1999). The HCV replicon system enabled investigation of anti-HCV reagents and the cellular factors involved in HCV RNA replication. Following introduction of the replicon system, genome-length HCV RNA-replication systems and reporter-assay systems were also developed (Ikeda *et al.*, 2002, 2005; Lohmann *et al.*, 2001; Pietschmann *et al.*, 2002). In 2005, an HCV infection system was developed using the genotype 2a JFH-1 strain (Lindenbach *et al.*, 2005; Wakita *et al.*, 2005; Zhong *et al.*, 2005). The JFH-1 infection system has been used to study not only viral RNA replication, but also virus infection and release. This HCV cell-culture system was developed using the human hepatoma cell line HuH-7 and, thus far, HuH-7 is the only cell line to exhibit robust HCV production. Therefore, we intended to test the susceptibility of various other cell lines to HCV RNA replication. We reported previously that the hepatoma cell line Li23 supports robust HCV RNA replication and is also susceptible to authentic JFH-1 infection (Kato *et al.*, 2009). Microarray analysis

†Present address: Center for AIDS Research, Kumamoto University, Kumamoto 860-0811, Japan.

Three supplementary figures are available with the online version of this paper.